

Fall colors have always been fascinating and are still a remarkably puzzling phenomenon associated with the breakdown of chlorophyll (Chl) in leaves. As discovered in recent years, nongreen bilin-type Chl catabolites are generated, which are known as the phyllobilins. Collaborative chemical-biological efforts have led to the elucidation of the key Chl-breakdown processes in senescent leaves and in ripening fruit. Colorless and largely photoinactive phyllobilins are rapidly produced from Chl, apparently primarily as part of a detoxification program. However, fluorescent Chl catabolites accumulate in some senescent leaves and in peels of ripe bananas and induce a striking blue glow. The structural features, chemical properties, and abundance of the phyllobilins in the biosphere suggest biological roles, which still remain to be elucidated.

1. Introduction

The rejuvenating appearance of chlorophyll (Chl) in spring and the seemingly pompous disappearance of the green plant pigments in the autumnal foliage of deciduous trees and bushes are very colorful natural phenomena. The seasonal breakdown of Chl, in particular, has always been enchanting, and also most puzzling. Indeed, Chl metabolism is probably the most visual sign of life on Earth, even observable from outer space.^[1] It has been estimated that more than 1000 million tons of the green plant pigment are biosynthesized and degraded every year on Earth.^[2] Once, it was believed that colored products would result from Chl breakdown, similar to the bilins from the breakdown of heme,^[3] or to photo-oxygenolysis products of Chl.^[4] Thus, all the early searches for Chl catabolites concentrated on the detection of such hypothetical colored leftovers of green Chl.^[5] As we now understand better, all of these endeavors were futile,^[1a,6] and Chl seemed to disappear without leaving a trace.^[2] Colored Chl catabolites were, indeed, not detected in higher plants, until very recently.^[7]

Only in the last 25 years^[8] has Chl breakdown in plants begun to reveal some of its molecular and cellular mysteries.^[1a,9] An original breakthrough was achieved by the unambiguous identification and structure elucidation of colorless Chl catabolites from vascular plants,^[1a,8,10] thereby paving the way for fundamental insights into Chl breakdown.^[9a,c,11] In distantly related studies, Kishi, Shimomura, and co-workers identified Chl-derived tetrapyrroles as luminescent compounds from marine photoorganisms.^[12] However, as became apparent in the early 1990s, these linear tetrapyrroles^[12] differed basically from the Chl catabolites from higher plants.^[8a,10]

1.1. A Breakthrough: Identification of a First Colorless Chl Catabolite from Higher Plants

By comparison of the pigment patterns of natural, wild-type senescent leaves of the grass *Festuca pratensis* and of barley (*Hordeum vulgare*) with the ones of corresponding

From the Contents

1. Introduction	4883
2. Chlorophyll Breakdown— a Cellular Three-Compartment Pathway	4885
3. Common Early Part of the PaO/Phyllobilin Pathway	4885
4. Branching of the PaO/ Phyllobilin Pathway in its Later Stages	4887
5. Chl Breakdown in <i>Arabidopsis thaliana</i> —A Model Case	4895
6. Long Overlooked Chl Catabolites in Fruit and Vegetables	4896
7. Phyllochromobilins from Oxidation of Phylloleucobilins	4897
8. Phyllobilins Are Natural Products with Remarkable Properties	4900
9. On the Role of Chlorophyll Breakdown in Higher Plants— Time for a New Paradigm	4901
10. Summary and Outlook	4902
11. Abbreviations	4904

“stay-green” mutants (that do not degreen), Matile, Thomas et al. were able to identify several colorless compounds that accumulated in senescent wild-type leaves, but were absent in the mutants.^[5,13] Some of these colorless compounds were suspected to be products of Chl breakdown. Several of them decomposed readily into rust-colored compounds and were called “rusty pigments”.^[14]

“Rusty pigment 14” (1) was a major colorless fraction in extracts of senescent primary leaves of barley, and suspected

[*] Prof. Dr. B. Kräutler
Institute of Organic Chemistry & Center of Molecular Biosciences
(CMBI), University of Innsbruck
6020 Innsbruck (Austria)
E-mail: bernhard.kraeutler@uibk.ac.at

ORCID(s) from the author(s) for this article is/are available on the WWW under <http://dx.doi.org/10.1002/anie.201508928>.

© 2016 The Authors. Published by Wiley-VCH Verlag GmbH & Co. KGaA. This is an open access article under the terms of the Creative Commons Attribution License, which permits use, distribution and reproduction in any medium, provided the original work is properly cited.

to be a Chl catabolite.^[14,15] ^{14}C -Labeled δ -aminolevulinic acid, the biosynthetic precursor of the natural porphyrinoids, was incorporated into the “rusty pigment 14” fraction, thereby providing further support for its presumed role as a Chl catabolite.^[15] Indeed, **1** could be identified as a Chl-derived linear tetrapyrrole^[8a] by a combination of mass spectrometry^[16] as well as UV/Vis, CD, and NMR spectroscopy.^[17] It was characterized as an optically active metal-free, colorless, and nonfluorescent linear tetrapyrrole with unconjugated pyrrole units. The linear tetrapyrrole **1** featured a Chl-diagnostic cyclopentanone unit, annealed to the α - and β -positions of a pyrrole ring, and carrying a methoxycarbonyl group. The colorless and nonfluorescent bilin-type tetrapyrrole **1** was, thus, identified as the first nongreen Chl catabolite from higher plants.^[11a,8a,9a]

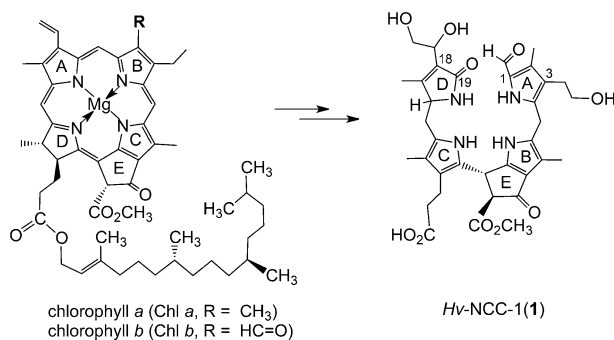


Figure 1. “Rusty pigment 14” from senescent leaves of barley (*Hordeum vulgare*), later named Hv-NCC-1 (**1**), was identified as the first nongreen Chl catabolite.^[8a]

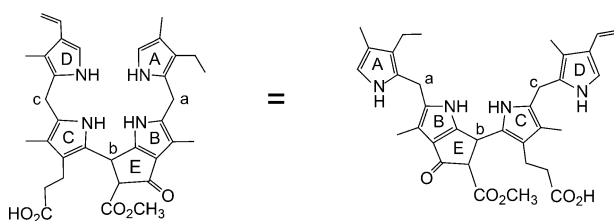


Figure 2. Phyllobilane (**1**),^[10] the name-giving structure, depicted in two representative formulas to highlight its pseudocyclic (left) and extended conformations (right).

The polar linear tetrapyrrole **1** from barley (*H. vulgare*) was classified as a nonfluorescent Chl catabolite (NCC), and provisionally named Hv-NCC-1.^[9a,18] Its detailed structure analysis established **1** as a 3²,18¹,18²-trihydroxy-16,19-dihydro-1-formyl-19-oxophyllobilane (Figures 1 and 2),^[8,19] named on the basis of a semisystematic, structure-based nomenclature, according to which linear tetrapyrrolic Chl catabolites are phyllobilin derivatives.^[9c,10] The “phyllobilin” terminus refers to the basic bilin-type structures of such Chl catabolites, and to chlorophyll as their origin. The name-giving compound is the phyllobilane (**1**, Figure 2). In analogy to the nomenclature of linear tetrapyrroles and bile pigments,^[3] NCCs with three saturated *meso* positions are, hence, classified as 16,19-dihydro-1-formyl-19-oxo-16-*epi*-phyllobilane (*epi*-**5**), identified in senescent leaves of the Katsura tree (*Cercidiphyllum japonicum*; see Table 1 in Section 4.1).^[20]

Structure elucidation of 1-formyl-19-oxophyllobilane **1** provided a first firm central focal point for considerations on the enigmatic pathway of Chl breakdown during leaf senescence:^[8a] The chemical constitution of **1** indicated loss of the central magnesium ion and of the phytyl group during breakdown of Chl. The structure of NCC **1** also implied an oxygenolytic opening of the porphyrinoid macrocycle at the northern *meso* position, thereby revealing a regioselectivity of Chl breakdown that was completely unexpected on the basis of model reactions with Chl derivatives.^[4b] It was reminiscent, in a striking way, of the breakdown of heme,^[3] in which the macrocycle of heme is also opened at the analogous α -*meso* position. However, in contrast to oxidation of the methine unit (of Chl) to the formyl group that is characteristic of NCC **1**, typical heme catabolites are 1,19-dioxobilins, which lack the carbon atom at the site of the cleavage of the macrocycle (which is removed as carbon monoxide by a reaction catalyzed by the heme oxygenase).^[21] As **1** carried a methyl group at its 2-position, it also appeared to be more closely related to Chl *a* than to Chl *b*.^[8a,22] However, compared to Chl *a*, additional polar functional units were attached at the periphery of **1**, thus rendering it rather soluble in water. Furthermore, the bilane-like **1** was indicated to exist in a variety of stable conformations with respect to its three saturated *meso* positions.

1.2. Nonfluorescent Chl Catabolites Accumulate in Senescent Leaves

The initially identified Hv-NCC-1 (**1**) was obtained from leaves that degreened upon storage in the dark. The use of this conventional method of artificially inducing leaf senescence raised the question of the more general validity of the surprising structure of the NCC **1**. Fortunately, Bn-NCC-1 (**2**), Bn-NCC-2 (**3**), and Bn-NCC-3 (**4**; Figure 3), related polar NCCs in naturally senescent leaves of oilseed rape (*Brassica napus*), were soon identified, thereby substantiating the role of NCCs as colorless products of natural Chl breakdown.^[18a,23]



Bernhard Kräutler studied chemistry at the ETH in Zürich, where he received his PhD in 1976 working with Prof. Albert Eschenmoser. After postdoctoral studies with Prof. Allen J. Bard (University of Texas, Austin) and Prof. Nicholas J. Turro (Columbia University, New York), he returned to the ETH to start his own research group. In 1991 he became Full Professor of Organic Chemistry at the University of Innsbruck, and since October 2015 has been Professor Emeritus. His research interests include chlorophyll breakdown, the chemical biology of vitamin B₁₂, as well as functionalized fullerenes and porphyrinoids.

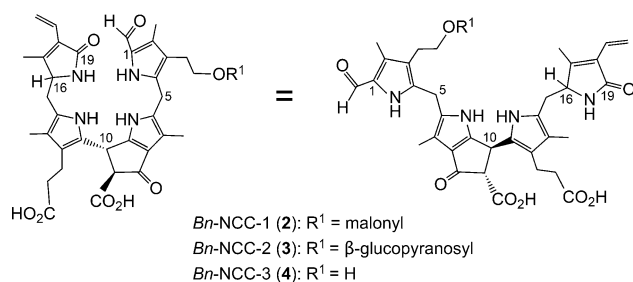


Figure 3. NCCs detected in naturally senescent cotyledons of *Brassica napus* (*Bn*-NCCs 2–4)^[23] depicted in representative formulas to highlight its pseudocyclic (left) and extended conformations (right).

2. Chlorophyll Breakdown—a Cellular Three-Compartment Pathway

Matile et al. found evidence for the localization of NCCs in the vacuoles.^[13c,24] Thus, catabolites of Chl, which originate in the chloroplasts, would need to pass through the cytosol to gain access to the vacuoles.^[9c,24] The breakdown of Chl was, therefore, proposed to involve metabolic processes in the three main compartments of leaf cells, including (unidirectional) transport between them.^[1a,9a] Subsequent research indicated an original fluorescent Chl catabolite (6, an FCC or 1-formyl-19-oxophyllobilene-*b*)^[25] as a colorless product of Chl breakdown in the chloroplasts. FCCs (similar to 6) were deduced to be exported into the cytosol, where further modified FCCs (*m*FCCs) would be generated.^[9c] Subsequently, typical *m*FCCs would be transported into the vacuoles to undergo rapid isomerization to the corresponding polar NCCs, lose their characteristic formyl group to furnish dioxobilin-type fluorescent Chl catabolites (DFCCs,^[26] the precursors of corresponding dioxobilin-type nonfluorescent Chl catabolites, DNCCs),^[26,27] or become persistent hypermodified FCCs (*hm*FCCs) that accumulate in leaves and fruit (and give the ripe bananas their blue glow; Figure 4).^[6b,28]

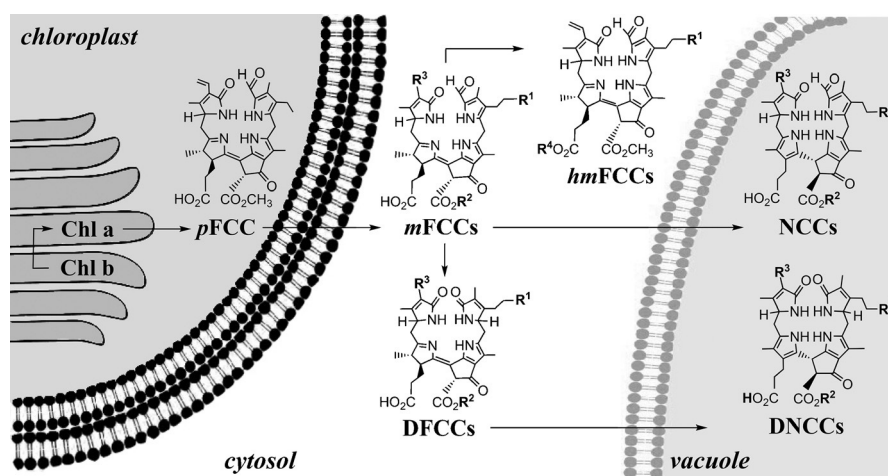


Figure 4. A simplified topographical model of Chl breakdown in a leaf cell, with relevant organelles and key types of Chl catabolites depicted.

Thus, a quarter of a century of collaborative chemical and biological research on Chl breakdown has not only revealed an unexpected structural variety of different natural Chl catabolites, but also key enzymes involved in the formation of the catabolites (see Sections 3 and 4).^[1a,8a,9a,c,10]

3. Common Early Part of the PaO/Phyllobilin Pathway

3.1. From Chlorophylls *a* and *b* to Pheophorbide *a*

The apparent close structural relationship of NCCs to Chl*a* raised the question of the whereabouts of the remains from the breakdown of Chl*b*. The observed specificity of the ring cleavage reaction for pheophorbide *a* (Pheo*a*) during Chl breakdown underlined this problem.^[29] However, isotopic labeling experiments by Folley and Engel with *Hv*-NCC-1 (1) showed significant incorporation of deuterium into the C2-methyl group of 1, thus supporting the origin of 1 from the degradation of both Chl*a* and Chl*b*, and suggesting the relevance of a reduction of the C2-formyl group of Chl*b*.^[30] Chl*a/b* interconversions were, indeed, revealed not only for the biosynthetic oxidative branch from chlorophyllide *a* to chlorophyllide *b*,^[31] but also its surprising reductive catabolic counterpart that converts Chl*b* back into Chl*a*, and involves 7¹-hydroxy-Chl*a* as an intermediate.^[32] In this way, a so-called Chl cycle^[11b,33] was shown to regulate the relative levels of Chl*a* and Chl*b* throughout the development of the plant, as well as in the initial stages of Chl breakdown in senescent plant tissues.^[9c,32]

Surprisingly, two different pathways are available in higher plants for the degradation of Chl*a* to Pheo*a* (Figure 5).^[9c] One of these, relevant in ripening citrus fruits, involves ester hydrolysis by chlorophyllase^[34] to give chlorophyllide *a* (Chlide*a*). This is followed by removal of the Mg ion to furnish Pheo*a*.^[35] However, this sequence is not functional in some senescent leaves, in which pheophytin *a* (Pheo*a*), the suggested product of direct Mg-removal from Chl*a*, was observed as an intermediate of Chl breakdown.^[36] In *A. thaliana*, the serine-type hydrolase pheophytinase was identified recently, which converts Pheo*a* into Pheo*a*, but does not hydrolyse Chl*a*.^[37] Thus, in senescent leaves of several plants, *in vivo* removal of the Mg ion from Chl*a* occurs first, followed by hydrolysis of the phytol ester.^[9c]

3.2. The Red Chlorophyll Catabolite—The Native Phyllobilin

The intriguing structures of NCCs (1-formyl-19-oxo-phyllobilanes) as late breakdown products called for the identification of earlier

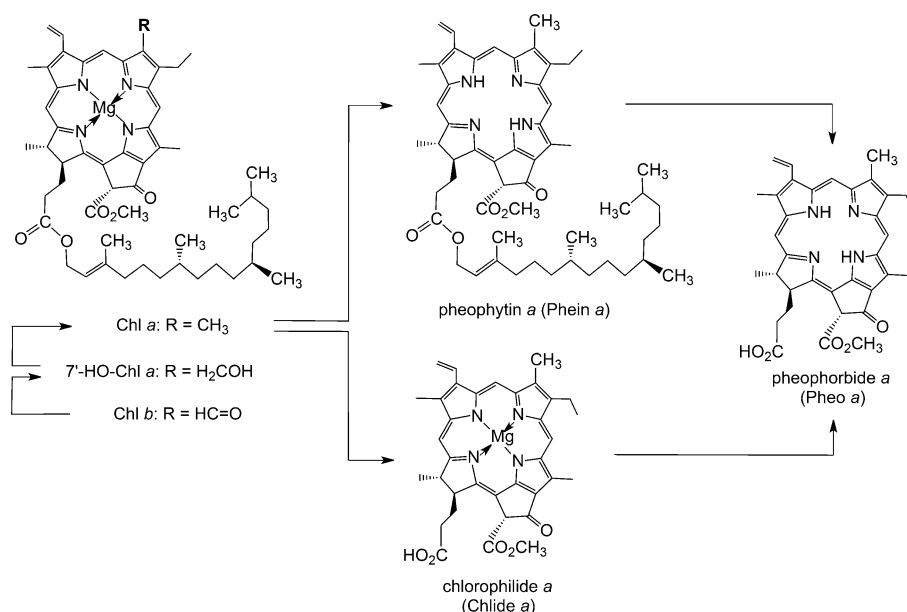


Figure 5. Early steps of Chl breakdown in the chloroplasts produce pheophorbide *a* (Pheo*a*).

intermediates of Chl degradation.^[38] Lipofuscin-like fluorescing compounds that could be identified in extracts of senescent leaves due to their blue fluorescence were suspected to be intermediate products of Chl breakdown.^[39] The blue-fluorescing compound **6** (originally named *Bn-FCC-2*) was first prepared from Pheo*a* by the use of an enzyme-active extract of senescent leaves of oilseed rape (*Brassica napus*).^[25] Its molecular formula (C₃₅H₄₀N₄O₇)^[40] confirmed a close relationship to Pheo*a*, with net addition of two O atoms and of four H atoms. Blue-fluorescing *Bn-FCC-2* (**6**) was, thus, proposed to be an intermediate of Chl breakdown and suggested to represent a product of Pheo*a* oxygenolysis.^[25] Pheo*a*, indeed, appeared to be degraded in a process requiring molecular oxygen.^[29] Furthermore, since Pheo*a* accumulated in leaves in the absence of oxygen, but not Pheo*b*, Pheo*a* was considered the last green intermediate of Chl breakdown in senescent leaves.^[29] This role of Pheo*a* required reduction of Chl*b* to Chl*a* as an early step of Chl breakdown.^[31,33]

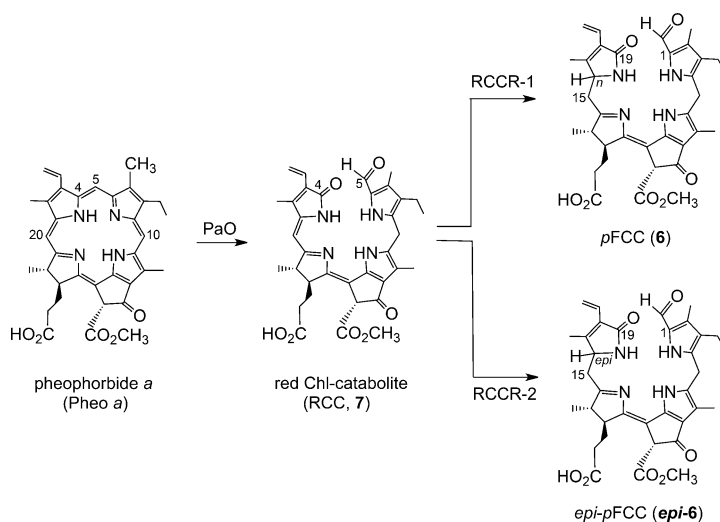


Figure 7. Chl breakdown from Pheo*a* via RCC (**7**) to primary FCCs (**6**/*epi-6*) is catalyzed by Pheo*a* oxygenase (PaO) and by two classes of RCC reductases (RCCR-1 and RCCR-2).^[3c]

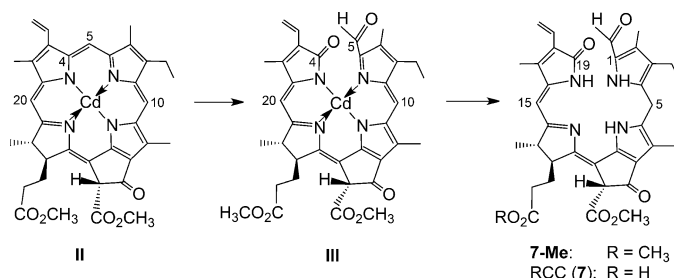


Figure 6. Photooxidation of the Cd^{II}-pheophorbide **II** and reduction of the 4,5-dioxocophytopyrhyrin **III** furnishes RCC (**7**) via its methyl ester precursor **7-Me**.^[42]

dihydro-1-formyl-19-oxophyllobiladiene-*b,c* **7** (now commonly called red Chl catabolite, RCC) was prepared from Pheo*a* by partial chemical synthesis.^[42] In analogy to experiments by the Gossauer research group with Cd^{II} complexes of pyropheophorbide *a* (13²-desmethoxycarbonyl-Pheo*a*),^[43] the Cd^{II} complex of Pheo*a* methyl ester (**II**) was photooxidized to furnish Cd^{II}-[4,5]-dioxo-[4,5]-seco-4,5-dihydromethylpheophorbide **III** in about 30% yield (Figure 6). The brownish and rather unstable oxidation product was readily reduced with NaBH₄ to give the deep-red RCC methyl ester (**7-Me**).^[42] Enzymatic hydrolysis of **7-Me** with porcine liver esterase selectively generated a first sample of authentic RCC (**7**) nearly quantitatively.^[42]

When synthetic **7** was available as a reference, traces of the very same (previously elusive) red compound were detected when *Pheoa* was incubated with extracts of chloroplasts of senescent *Brassica napus* cotyledons.^[44] Indeed, RCC was eventually revealed as the product of a Rieske-type monooxygenase, named *Pheoa* oxygenase (PaO),^[45] that uses *Pheoa* selectively as its substrate and that is inhibited by *Pheob.*^[46] Therefore, RCC (**7**) carries the hallmarks of the oxygenolytic ring opening by PaO, considered the key step of the PaO/phytylobilin pathway of Chl breakdown (Figure 7).^[9c,29,46] In this enzyme-catalyzed process, the chlorin-type macroring of *Pheoa* is cut open between C4 and C5, and one oxygen atom is specifically incorporated into the newly produced, characteristic formyl group of (an enzyme-bound form of) RCC (**7**).^[46] Thus, RCC (**7**) is the native 1-formyl-19-oxobilin-type Chl catabolite, or native phytylobilin.

3.3. Primary Fluorescent Chl Catabolites—Epimeric Pair of Phytylobilin Ancestors

Synthetic RCC (**7**) was shown in extracts of senescent *B. napus* leaves to be reduced to the presumed Chl catabolite **6**, provisionally called *Bn*-FCC-2.^[44] NMR spectroscopic studies^[17] had already shown that *Bn*-FCC-2 (**6**) was a 12,13,16,19-tetrahydro-1-formyl-19-oxophytylobilene-*b* (Figure 7). As **6** exhibited the same pattern of peripheral functional groups as *Pheoa*, and was not modified further by polar groups known from the NCC structures, it was called the primary FCC (*p*FCC).^[25] In addition to the characteristic absorption maximum of an α -formylpyrrole unit (ring A) near $\lambda = 315$ nm,^[8a] the UV/Vis spectra of **6** showed a new maximum at $\lambda = 360$ nm, corresponding to a new chromophore extending over rings B and C (Figure 8).^[6b,25] In contrast to the nonluminescent NCCs, solutions of FCC **6** exhibit a strong and characteristic blue fluorescence, with an emission maximum near $\lambda = 450$ nm. It was this feature that led to the original phenomenological classification as an FCC.^[6b,25]

By using an aerated enzyme assay based on a suspension of chromoplasts of red sweet pepper (*Capsicum annuum*),

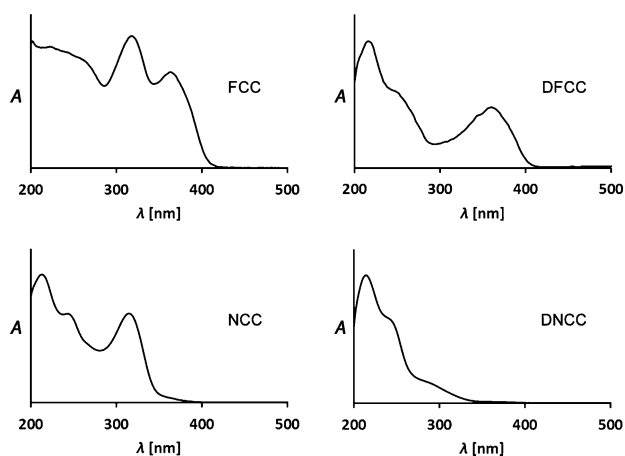


Figure 8. UV spectra of representative colorless phytylobilins of type-I (FCC and NCC) and of type-II (DFCC and DNCC).^[26a]

Pheoa was transformed into another blue-fluorescing compound, originally called *Ca*-FCC-2, and identified as an isomer of *p*FCC (**6**).^[47] Detailed NMR-spectroscopic analysis indicated a configurational difference between **6** and *Ca*-FCC-2 at C16 (C1 in the earlier phytyporphyrin-based nomenclature^[47]). *Ca*-FCC-2 was, therefore, named *epi-p*FCC (*epi-6*, Figure 7).^[47]

Reduction of RCC (**7**) to *p*FCC (**6**) was shown to be accomplished by a cofactor-free RCC reductase (RCCR).^[48] The identification of **6** and its C16 epimer *epi-6* suggested two stereospecific classes of RCCRs in higher plants. This conclusion was verified by studies of the RCCRs from a range of plants and their classification as RCCR-1 and RCCR-2.^[49] RCCR of *B. napus* is a RCCR-1 and achieves a highly stereo- and regioselective reduction of RCC (**7**) to *p*FCC (**6**).^[25,48] The same (regio- and) stereoselectivity is deduced for RCCRs from some other plants, among them *A. thaliana*.^[49b] In contrast, in a second group of plants, among them spinach (*Sp. oleracea*)^[50] and bananas (*M. acuminata*),^[51] C16-epimeric NCCs were found as descendants of *epi-p*FCC (*epi-6*) from the reduction of RCC (**7**) by an enzyme of the RCCR-2 class.^[49a] RCC reductase (RCCR) is a constitutively expressed enzyme, now classified as belonging to the family of the (ferredoxin-dependent) bilin reductases.^[52] The crystal structure of RCCR from *A. thaliana* was analyzed in substrate-free and RCC-loaded forms (see Refs. [53,54] for structural details).

3.4. Partial Synthesis of *p*FCC and *epi-p*FCC—A Chemical Interlude

Controlled-potential electrolytic reduction of RCC methyl ester (**7-Me**) in a protic solvent system furnished FCC methyl esters **6-Me** and *epi-6-Me* in about 25% yield, and with negligible stereoselectivity.^[55] This (chemical) reaction represented a first model process for the reaction catalyzed by the cofactor-free RCCRs, exploring the ease of the one-electron reduction of **7-Me**. Likewise, *p*FCC (**6**) and *epi-p*FCC (*epi-6*) were similarly obtained by electrochemical reduction of synthetic RCC (**7**), and revealed useful regioselectivity for the addition of hydrogens at the 15- and 16-positions, but an absence of significant stereoselectivity (Figure 9).^[20b] Hence, this experiment provided access to both C16 epimers of the natural primary FCCs.

The facile electrochemical reduction of **7** to **6** and *epi-6* in weakly acidic solution was in line with a ferredoxin-driven reduction^[54,56] catalyzed by RCCRs. Indeed, enzymatic reduction of RCC (**7**) by RCCR was deduced to follow a related mechanistic sequence, through protonation and single electron transfer reduction steps.^[54]

4. Branching of the PaO/Phytylobilin Pathway in its Later Stages

Degreened leaves of barley (*H. vulgare*) were not only the first source of the colorless NCC **1**, but also of a second major type of nonfluorescent and colorless Chl catabolites, the

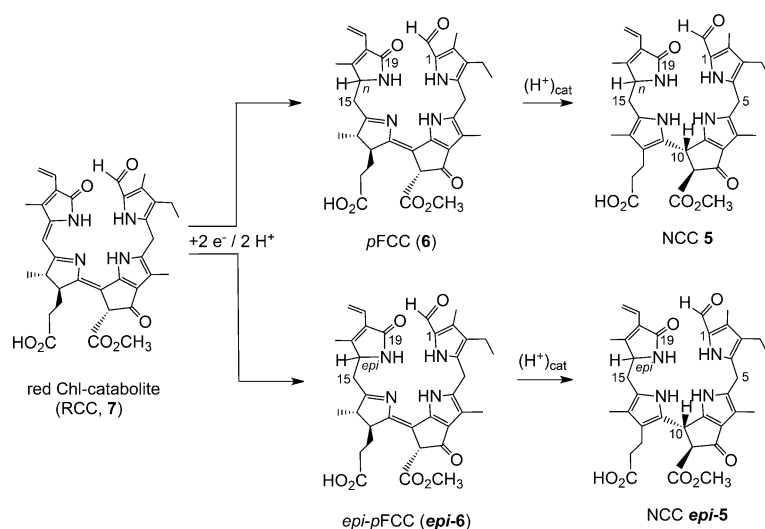


Figure 9. Bio-inspired partial chemical synthesis of the NCCs **5** and **epi-5** by electrochemical reduction of RCC (**7**) to **pFCC** and **epi-pFCC** (**6** and **epi-6**), followed by stereoselective acid-catalyzed isomerization to **5** and **epi-5**.^[20b]

urobilinogenoidic Chl catabolites (UCCs) **8a** and **8b**.^[57] The two epimers, **8a** and **8b**, found in the barley leaf extracts, appeared to be direct descendants of *Hv*-NCC-1 (**1**).^[57] However, consistent with the absence of a formyl group, the UV spectra of these phyllobilins lacked the absorption band near $\lambda = 315$ nm, which is typical of NCCs, such as **1**. The

tetrapyrroles **8a** and **8b** are now classified, in a structure-based way, as 1,19-dioxobilin-type NCCs (DNCCs, Figure 10).^[10] More recently, the major colorless phyllobilin in senescent leaves of Norway Maple (*Acer platanoides*) was also characterized as a DNCC, and shown by its CD spectra to behave as the enantiomer (**ent-8a**) of the barley DNCC **8a**.^[58] This striking finding led to the suggestion that DNCCs may not be derived from NCCs, but would probably originate from an earlier Chl-breakdown intermediate, thus basically indicating a divergent pathway of Chl breakdown (see Section 4.2).^[58]

1-Formyl-19-oxobilin-type Chl catabolites only appear to be present in a variety of senescent leaves and ripe fruit, such as spinach leaves,^[50] apples, and pears.^[59] In striking contrast, only the remarkable 1,19-dioxobilin-type Chl catabolite **ent-8a** was detected in senescent leaves of Norway maple.^[58] However, both lines of colorless phyllobilins were present in senescent leaves of *Arabidopsis thaliana*^[27,60] and in broccoli florets (*B. oleracea*).^[61]

As we now know, 1,19-dioxobilin-type Chl catabolites (DCCs), which have in the meantime been classified as type-II phyllobilins, branch off from the original lineage of the 1-formyl-19-oxophyllobilins, or type-I phyllobilins. Branching occurs at the stage of FCCs, where oxidative deformylation competes with pathways to other downstream type-I phyllobilins (*hm*FCCs, NCCs) and leads mainly to 1,19-dioxobilin-type NCCs (DNCCs).^[10,26a] Two such branching points have, so far, been identified in *A. thaliana* (Figure 11).^[26c]

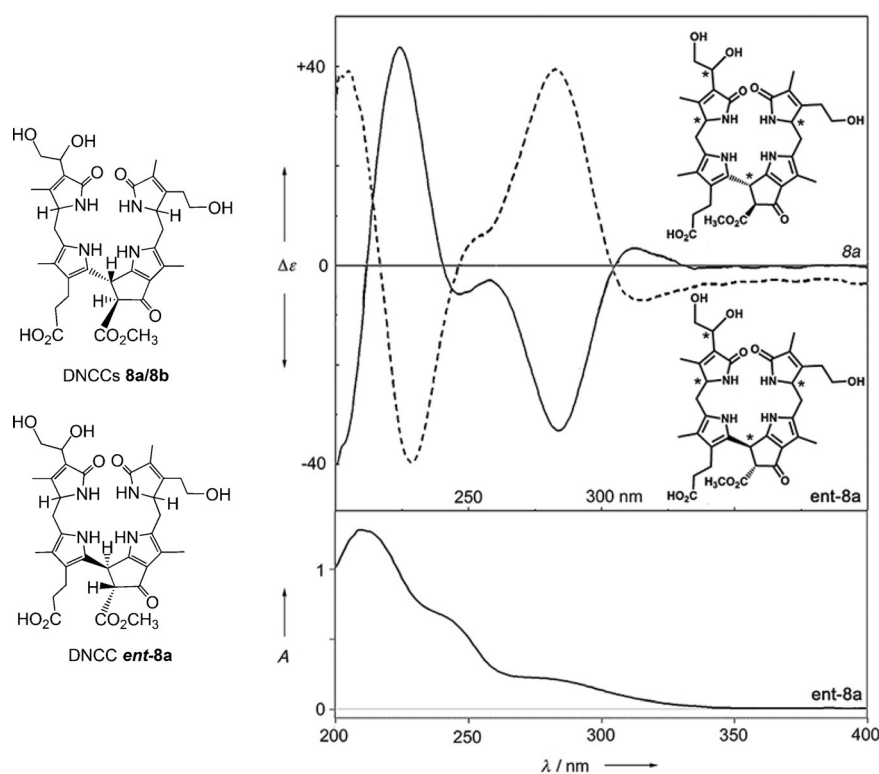


Figure 10. Structural formulas (left) of DNCCs **8a/8b** (from barley)^[57] and **ent-8a** (from a Norway maple leaf),^[58] whose CD and UV spectra (right) feature the properties of an intriguing enantiomer of **8a**.

4.1. The Original Type-I Phyllobilins—Colorless 1-Formyl-19-oxobilins

Over the years, about 20 structurally different natural (nonfluorescent) 1-formyl-19-oxophyllobilanes (NCCs or type-I phylloleucobilins) have been characterized, firmly establishing their broad relevance as final Chl catabolites in senescent leaves of various plants. Among these were, for example, the NCCs **1–4** (see Sections 1 and 2), **epi-9** and **epi-10** from tobacco (*Nicotiana rustica*^[62]), **epi-5** and **epi-11** from *C. japonicum*^[20a,63], **epi-1**, **epi-5**, **epi-11**, **epi-12**, and **epi-13** from spinach^[50,64] (*Spinacia oleracea*), **epi-9** and **epi-14** from maize^[65] (*Zea mays*), as well as **3**, **4**, **15–17** from *A. thaliana*^[60,66] (see Table 1 and Figure 12).^[10] NCCs were identified tentatively in extracts of senescent leaves on the basis of their characteristic UV-absorption maximum near $\lambda =$

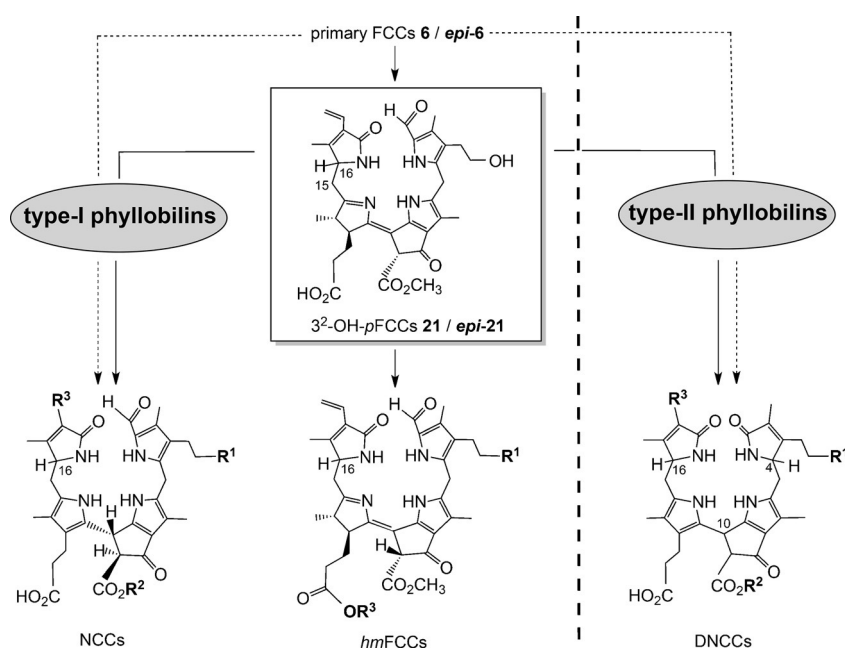


Figure 11. Branching of Chl breakdown occurs at the level of FCCs and provides pathways to downstream type-I and type-II phyllobilins (see Tables 1–3 for examples of R^1 , R^2 , and R^3).^[10]

315 nm (Figure 8).^[8] ESI-MS spectra helped to establish the molecular formula. Characteristic fragments often allowed conclusions concerning functional groups.^[16c] The ^1H NMR spectra of NCCs show a characteristic singlet corresponding to the $\text{CH}=\text{O}$ group at low field.^[8a] The constitution of the phyllobilins and part of their relative configuration was deduced from analysis of high-field ^1H , ^1H homonuclear and ^1H , ^{13}C heteronuclear NMR spectra.^[8a,10,17a]

All NCCs (or 16,19-dihydro-1-formyl-19-oxophyllobilanes^[10]) are flexible linear tetrapyrroles with unconjugated pyrrolic units. As descendants of *pFCC* (**6**) or *epi-pFCC* (*epi-6*), which differ by their absolute configuration at C16 in a species-specific way, NCCs also occur in two epimeric classes (see, for example, Ref. [64] and Table 1). With one striking exception, NCCs carry a methyl group at C2.^[10] The noted exception is *At-NCC-3* (**15**, from senescent leaves of *A. thaliana*), in which a hydroxymethyl group is attached at C2.^[66] Furthermore, all NCCs, and other known natural phyllobilins from

Table 1: Structures of natural 1-formyl-19-oxophyllobilanes or nonfluorescent Chl catabolites (NCCs).

No. ^[a]	R^1 ^[b]	R^2 ^[b]	R^3 ^[b]	C16 ^[c]	Original name (identical with) ^[d]	Ref.
17	H	H	$\text{CH}=\text{CH}_2$	n	<i>Bo-NCC-2</i> (<i>At-NCC-5</i> / <i>Bn-NCC-4</i> ^[6])	[60, 61]
15	H	H	$\text{CH}=\text{CH}_2$	n	<i>At-NCC-3</i> ^[f]	[66]
<i>epi-5</i>	H	CH_3	$\text{CH}=\text{CH}_2$	epi	<i>Cj-NCC-2</i> (<i>So-NCC-5</i>)	[20a, b50]
4	OH	H	$\text{CH}=\text{CH}_2$	n	<i>Bn-NCC-3</i> (<i>At-NCC-2</i> ^[6])	[23, 60]
<i>epi-13</i>	OH	H	$\text{CH}=\text{CH}_2$	epi	<i>So-NCC-3</i> (<i>Mc-NCC-49</i> / <i>Ej-NCC-3</i> ^[6])	[50, 51, 83]
<i>epi-12</i>	OH	H	$\text{CH}(\text{OH})-\text{CH}_2\text{OH}$	epi	<i>So-NCC-1</i> (<i>Mc-NCC-26</i>)	[50, 51]
11	OH	CH_3	$\text{CH}=\text{CH}_2$	n	<i>Sw-NCC-58</i>	[91]
<i>epi-11</i>	OH	CH_3	$\text{CH}=\text{CH}_2$	epi	<i>Cj-NCC-1</i> (<i>So-NCC-4</i> / <i>Pc-NCC-2</i> / <i>Md-NCC-2</i> / <i>Mc-NCC-61</i> / <i>Ej-NCC-4</i> ^[6])	[50, 51, 59, 63] [83]
1	OH	CH_3	$\text{CH}(\text{OH})-\text{CH}_2\text{OH}$	n	<i>Hv-NCC-1</i>	[8]
<i>epi-1</i>	OH	CH_3	$\text{CH}(\text{OH})-\text{CH}_2\text{OH}$	epi	<i>So-NCC-2</i> (<i>Mc-NCC-42</i> / <i>Ej-NCC-1</i> ^[6])	[50, 51, 64, 83]
3	O-Glc	H	$\text{CH}=\text{CH}_2$	n	<i>Bn-NCC-2</i> (<i>At-NCC-1</i> ^[6] / <i>Bo-NCC-1</i>)	[23, 60, 61]
16	O-Glc	CH_3	$\text{CH}=\text{CH}_2$	n	<i>At-NCC-4</i> ^[6]	[60]
<i>epi-9</i>	O-Glc	CH_3	$\text{CH}=\text{CH}_2$	epi	<i>Nr-NCC-2</i> (<i>Zm-NCC-2</i> / <i>Pc-NCC-1</i> / <i>Md-NCC-1</i> / <i>Tc-NCC-2</i> / <i>Mc-NCC-59</i>)	[51, 59, 62, 65, 92]
<i>epi-14</i>	O-Glc	CH_3	$\text{CH}(\text{OH})-\text{CH}_2\text{OH}$	epi	<i>Zm-NCC-1</i> (<i>Tc-NCC-1</i> / <i>Co-NCC-1</i> ^[6])	[65, 82, 92]
<i>epi-18</i>	O-Glc	CH_3	$\text{CH}(\text{OH})-\text{CH}_2\text{O-Glc}$	epi	<i>Pd-NCC-32</i>	[68]
<i>epi-10</i>	O-MalGlc	CH_3	$\text{CH}=\text{CH}_2$	epi	<i>Nr-NCC-1</i>	[62]
2	O-Mal	H	$\text{CH}=\text{CH}_2$	n	<i>Bn-NCC-1</i>	[18a, 23]
<i>epi-29</i>	O-Mal	CH_3	$\text{CH}=\text{CH}_2$	epi	<i>Ej-NCC-2</i> ^[6]	[83]
<i>epi-20</i>	OH	CH_3	$\text{CH}=\text{CH}_2$	epi	<i>Mc-NCC-58</i> ^[6, h]	[51]
<i>epi-21</i>	OH	CH_3	$\text{CH}=\text{CH}_2$	epi	<i>Mc-NCC-55</i> ^[h, i]	[51]

[a] Compound number (see text). [b] R^1 to R^3 refer to a generalized NCC formula, shown in Figure 13. Abbreviations: Mal = malonyl; Glc = β -glucopyranosyl, MalGlc = O β -(Mal)Glc. [c] The absolute configuration of NCCs at C16 is still unknown; assigned as “n” or as “epi”, when the NCC is derived from *pFCC* (**6**) or from *epi-pFCC* (*epi-6*), respectively. [d] *Bo-NCCs*: *B. oleracea* var. *italica* (broccoli),^[61] *At-NCCs*: *A. thaliana*,^[60, 66] *Bn-NCCs*: *B. napus* (oilseed rape),^[18a, 23] *Cj-NCCs*: *C. japonicum* (Katsura tree),^[20a, 63] *So-NCCs*: *Sp. oleracea* (spinach),^[50, 64] *Mc-NCCs*: *M. acuminata* (banana peels, Cavendish cultivar),^[51] *Sw-NCC-58*: *Sp. wallisii* (Peace Lily),^[91] *Pc-NCCs*: *P. communis* (pear),^[59] *Md-NCCs*: *M. domestica* (apple),^[59] *Hv-NCC-1*, *H. vulgare* (barley),^[8] *Nr-NCCs*: *N. rustica* (tobacco),^[62] *Zm-NCCs*: *Z. mays* (maize),^[65] *Tc-NCCs*: *T. cordata* (lime tree),^[92] *Ej-NCCs*: *E. japonica* (loquat fruits),^[83] *Co-NCCs*: *C. oblonga* (quince),^[82] and *Pd-NCCs*: *P. domestica* (plum tree).^[68] [e] Tentative assignments based on UV/Vis and mass spectra. [f] *At-NCC-3* (**15**) carries a HOCH_2 group at C2.^[66] [g] *R* Configuration at C10 derived from the CD spectrum.^[51] [h] *S* Configuration at C10 derived from the CD spectrum.^[51] [i] propionate side chain esterified with a daucyl unit.^[28a, 85]

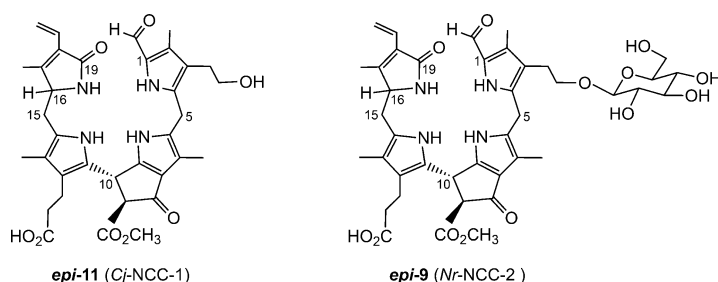


Figure 12. Constitutional formulas of two common natural NCCs. Catabolites **epi-11** and **epi-9** (first identified as *Cj*-NCC-1 and *Nr*-NCC-2, respectively), which are also present in the peels of apples and pears (see Table 1).

higher plants, feature a methoxycarbonyl group or a carboxy group at their C8²-position (Table 1). This structure of ring E excludes pyropheophorbide *a* (13²-desmethoxycarbonyl-Pheo*a*) as a rational biological precursor of natural NCCs.

The amphiphilic NCC 3²-hydroxy-16,19-dihydro-1-formyl-19-oxo-*epi*-phytylobilane (**epi-11**) has been encountered in various higher plants,^[6a] for example, as *Cj*-NCC-1 in leaves of *C. japonicum*.^[20a,63] It carries a hydroxyethyl group at the C3-position of ring A, which increases its polarity. The phyllobilane **epi-11** was also described, for example, as *Pc*-NCC-2 and as *Md*-NCC-2 in senescent leaves of pear and apple trees, as well as in the corresponding ripe fruit.^[59] Its epimer, the 3²-hydroxy-16,19-dihydro-1-formyl-19-oxo-epi-phytylobilane **11**, was detected (as *So*-NCC-4) in senescent spinach leaves and (as *Sw*-NCC-58) in Peace Lily (*Spathiphyllum wallisii*) leaves. The 3²-OH group may serve as an anchor for further attachment of hydrophilic groups at this position. Thus, the 3²-(β -glucopyranosyl)oxy-1-formyl-19-oxo-*epi*-phytylobilane (**epi-9**) was discovered in senescent tobacco leaves and originally named *Nr*-NCC-2.^[62] Constitutional variability in 1-formyl-19-oxo-epi-phytylobilanes (or NCCs, see Table 1) was found in the side chains at positions C3, C8, and C18, all resulting from peripheral modifications during catabolism by malonylation,^[18a] methyl ester hydrolysis,^[23,67] and/or dihydroxylation of the C18 vinyl group.^[8a] Unique NCC structures were recently identified in leaves of plum trees (*Prunus domestica*), where *Pd*-NCC-32 (**epi-18**) is glycopyranosylated twice (at O3³ and O18³),^[68] as well as in leaves of Wich Elm (*Ulmus glabra*), where a bridging glucopyranosyl group generated an unprecedented [17.3.1] bicycloglycosyl motif in *Ug*-NCC-3 (**19**; Figure 13).^[69] In addition, traces of other unprecedented, natural NCC esters (*Mc*-NCC-58, **epi-20** and its C10 epimer *Mc*-NCC-55, **epi-21**) were identified from peels of ripe bananas by comparison of the HPLC traces with those of authentic reference material obtained from acid-catalyzed isomerization of *Mc*-FCC-56 (see Section 6).^[51] Thus, the NCC structures suggested a range of enzyme-catalyzed reactions relevant in Chl degradation in senescent leaves, such as hydroxylation, glycosylation, malonylation,^[70] dihydroxylation, methyl ester hydrolysis,^[67] and formation of propionate esters. Hydroxylation at C3²^[51] and hydrolysis of the methyl ester function at O8⁴^[60,67] were deduced to occur with the corresponding FCC precursors. Likewise, glycosylation, malonylation, ester formation, and side chain dihydrox-

ylation, observed in some NCCs, are also expected to involve enzyme-catalyzed reactions of FCCs. Indeed, modified FCCs (*m*FCCs) with structures reflected by the functional groups observed in NCCs^[10] appear to be functionalized with their respective polar groups before entering the vacuole and undergoing direct isomerization to NCCs there.^[9c,20a]

The fluorescent Chl catabolites (FCCs or 12,13,16,19-tetrahydro-1-formyl-19-oxo-epi-phytylobilanes) and corresponding (nonfluorescent) NCCs (16,19-dihydro-1-formyl-19-oxo-epi-phytylobilanes) are isomers. This structural relationship suggested that FCCs could isomerize into NCCs,^[20a] driven by aromatization of ring C to a pyrrole unit, as seen in hydroporphyrins.^[71]

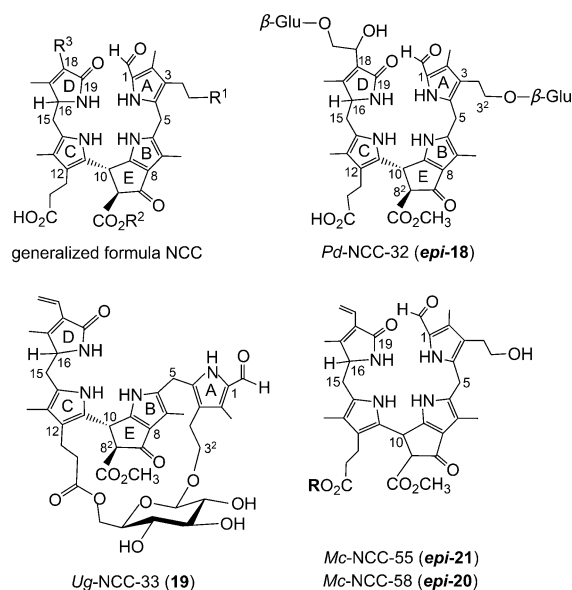


Figure 13. Generalized NCC formula, including atom numbering (top left) and structural formulas of natural NCCs with unique structures: doubly glycosylated *Pd*-NCC-32 (**epi-18**), bicycloglycosidic *Ug*-NCC-3 (**19**), and epimeric NCC esters **epi-20/epi-21** from banana peels (*R* = daucyl unit, *Mc*-NCC-58 has an *R* configuration at C10, *Mc*-NCC-55 is the *S* epimer).

The hypothetical non-enzymatic isomerization of FCCs to NCCs was tested with both primary FCCs, **6** and **epi-6**.^[20a,b] First, an acid-induced isomerization of *epi*-pFCC (**epi-6**) was studied, which converted **epi-6** into the natural *Cj*-NCC-2 (**epi-5**) with high stereoselectivity.^[20a] Isomerization of **epi-6** to **epi-5** (Figure 9) was rapid at pH 4.9, and **epi-6** had a half-life of less than 30 min.^[20a] Likewise, at pH 4.0, the pFCCs **6** and **epi-6** isomerized stereoselectively to the respective epimeric NCCs **5** and **epi-5** (Figure 9), with apparent first-order rate constants of 0.020 and 0.039 min⁻¹, respectively.^[6b,20b]

Consistent with their rapid isomerization to NCCs, typical FCCs can only be observed fleetingly in senescent plant material. The free propionic acid group at C12 of ring C activates and steers the (acid-induced) FCC to NCC isomerization in a remarkably stereoselective way^[20b] (see Ref. [20a] for a mechanistic discussion). Indeed, a pH profile of the reaction rate was consistent with the participation of a proton donor with a p*K*_a value of about 5, thus supporting the

mechanistic view that the isomerization was achieved by an intramolecular protonation of C10 by the propionic acid function. A second carboxylic acid group at the C8²-position of the natural polar *At*-FCC-2 (**22**) further accelerated the FCC to NCC isomerization by a factor of about 7 at pH 5 (a probable consequence of a local charge effect).^[67] Therefore, a non-enzymatic isomerization of FCCs to NCCs was proposed to account for the formation of NCCs in the acidic milieu of the vacuoles, where the free propionic acid function would be partially protonated. The intramolecular protonation step was deduced to preferentially generate NCCs with an *R* configuration at C10. Consistent with the proposed chemical mechanism of the isomerization of natural FCCs to the corresponding NCCs, natural NCCs basically exhibit—with few exceptions—similar CD spectra, thus supporting their common absolute configuration at the (C10) *meso* position between pyrrole rings B and C.^[20a,b] The deduced *R* configuration of the NCC *epi-11* at C10 was recently confirmed by detailed structural analysis, including X-ray analysis, of a yellow Chl catabolite (YCC) derived from this NCC (see Section 7).^[72]

The critical role of the propionic acid side chain in the FCC to NCC isomerization was further demonstrated by studying this type of isomerization reaction with the related FCC methyl esters **6-Me** and *epi-6-Me*, which were obtained from partial synthesis.^[20b] Both epimeric *p*FCC esters eventually isomerized to the corresponding NCC methyl esters,

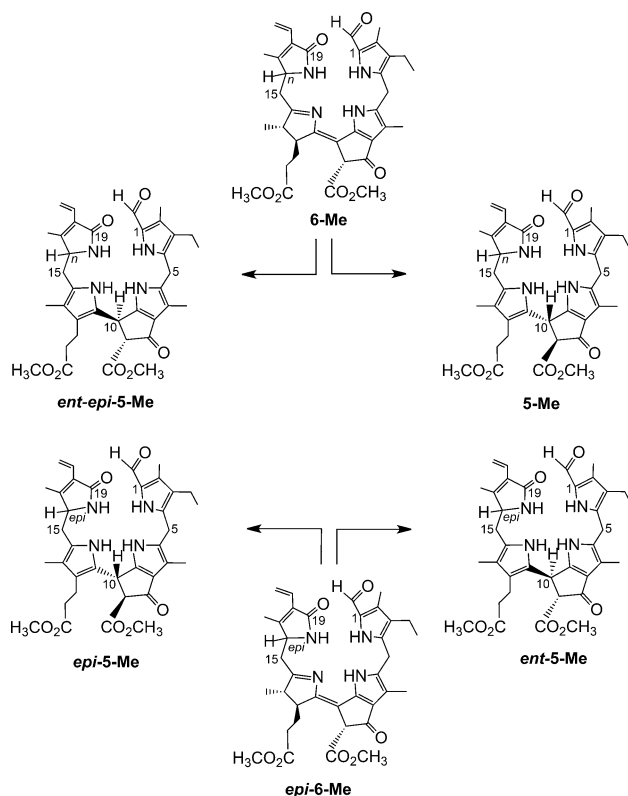


Figure 14. Acid-induced isomerization of methyl esters of primary FCCs (**6-Me/epi-6-Me**) to NCCs is slow and lacks significant stereoselectivity; it furnishes methyl esters of their normal and epi lineages **5-Me/epi-5-Me**, as well as of both of their enantiomers (*ent-5-Me/ent-epi-5-Me*).^[20b]

but with low stereoselectivity at C10, slow reaction rate, and low conversion (**5-Me/ent-epi-5-Me** from **6** and *epi-5-Me/ent-5-Me* from *epi-6-Me* Figure 14).^[20b] Thus, the mirror images of both natural type NCCs are easily accessible (as methyl esters). Clearly, activation of the isomerization by the free propionic acid function is blocked by its esterification. This remarkable finding has helped to rationalize the surprising accumulation of persistent FCCs in ripening bananas (see Section 6), which are FCCs, biologically “caged” with a propionate ester function.^[28a]

So far, natural NCCs were deduced to feature a common *R* configuration at C10. However, two NCCs, recently isolated from leaves of birch trees displayed CD spectra that were essentially mirror images of the CD spectrum of **1**, thus suggesting a reversed configuration at C10.^[73] This finding suggests, first of all, the relevance of alternative ways that may generate NCCs with the reversed configuration at C10. Possibly, the FCC to NCC isomerization is achieved by an enzyme-controlled, stereochemically different process in birch leaves. The observation of the aberrant configuration in birch NCCs emphasizes the importance of CD spectra for the characterization of new NCCs.

Various colorless fluorescent Chl catabolites (FCCs), or type-I phyllochromobilins, were detected in extracts of senescent leaves, where they are easily traced by their (blue) fluorescence. As described above, the primary fluorescent Chl catabolites are formed in higher plants by direct enzyme-catalyzed reduction of protein-bound RCC (**7**). The absolute configuration at the C16-position of the epimeric primary FCCs **6**^[10,25] and *epi-6* could, so far, not be specified.^[21a,47] Therefore, FCCs are classified as belonging either to the normal series (for **6** and *m*FCCs derived from **6**) or to the epi series (*epi-6* or *m*FCCs derived from *epi-6*). The configuration at C16, once introduced at the *p*FCC level, appears to be retained under physiological conditions in *m*FCCs and in their descendants (NCCs, DNCCs, etc.). Therefore, NCCs, DNCCs, etc. also belong either to the normal or to the epi series (Tables 1 and 2 in this section and Table 3 in Section 4.2).

In contrast to the often accumulating NCCs, and with the exception of the unusually persistent hypermodified FCCs (see Section 6),^[28a] typical FCCs exist only fleetingly in leaves of senescent plants, and their structures have only occasionally been assigned.^[10] In addition, primary FCCs appear to be rapidly functionalized further, and the hydroxylation of *p*FCC/*epi-p*FCC at the C3²-position is an early event in Chl breakdown in higher plants, probably taking place in the chloroplasts.^[9c] Consistent with such an early and efficient hydroxylation at the C3²-position in senescent leaves, 3²-hydroxy-1-formyl-19-oxophyllobilanes (NCC **11** or its C16 epimer, *epi-11*) are a typical major NCC fraction in extracts of senescent leaves, but the corresponding analogues lacking the 3²-OH group were not (**5**) or were only rarely (*epi-5*) detected.^[20a] However, naturally formed *p*FCC (**6**) was detected (as *At*-FCC-3) in extracts of senescent *A. thaliana* leaves.^[60] 3²-Hydroxy-*p*FCC (**23**, 3²-hydroxy-12,13,16,19-tetrahydro-1-formyl-19-oxophyllobilene-*b*) was likewise found in senescent leaves of the methyl esterase mutant (MES16) of *A. thaliana*, in which activity for the hydrolysis of the methyl

ester function of phyllobilins is lacking.^[67] Its epimer, 3²-hydroxy-*epi-p*FCC (**epi-23**, 3²-hydroxy-12,13,16,19-tetrahydro-1-formyl-19-oxo-*epi*-phyllobilene-*b*), was identified as *Mc*-FCC-62 in the peels of ripening bananas.^[51] Two additional polar FCCs were tentatively identified in senescent *A. thaliana* leaves: 3²-hydroxy-O⁸-desmethyl-12,13,16,19-tetrahydro-1-formyl-19-oxophyllobilene-*b* (*At*-FCC-1, **24**) and O⁸-desmethyl-12,13,16,19-tetrahydro-1-formyl-19-oxophyllobilene-*b* (*At*-FCC-2, **22**), which are formed by hydrolysis^[67]

of the Chl in a green leaf) was found in naturally degreened leaves of the tropical evergreen *Spathiphyllum wallisii*.^[74] This hypermodified FCC (*hm*FCC), named *Sw*-FCC-62 (**25**), was esterified with a β -glucopyranosyl-(1 \rightarrow 1)-2-(3,4-dihydroxyphenyl)ethyl group at the crucial propionyl side chain extending from C12 (Figure 16). As propionate ester functions stabilize *hm*FCCs against their acid-induced isomerization to NCCs, *hm*FCCs are a remarkable group of biologically “caged” versions of ordinary FCCs.

Table 2: Structures of natural fluorescent type-I phyllobilins (FCCs, top section) and type-II phyllobilins (DFCCs, *iso*-DFCC, bottom section): labels R¹, R², and R⁴ refer to the generalized formula of FCCs (with atom numbering), shown in Figure 15.

No. ^[a]	R ¹	R ²	R ⁴	C16 ^[b]	Provisional names ^[c]	Ref.
22	H	H	H	n	<i>At</i> -FCC-2	[60]
6	H	CH ₃	H	n	<i>Bn</i> -FCC-2 (<i>p</i> FCC)	[25, 60]
epi-6	H	CH ₃	H	epi	<i>Ca</i> -FCC-2 (<i>epi-p</i> FCC)	[47]
24	OH	H	H	n	<i>At</i> -FCC-1	[60]
23	OH	CH ₃	H	n	3 ² -OH- <i>p</i> FCC	[27]
epi-23	OH	CH ₃	H	epi	<i>Mc</i> -FCC-62	[51]
23-Me	OH	CH ₃	CH ₃	epi	<i>Mc</i> -FCC-71 ^[e]	[51]
epi-41	OH	CH ₃	5'-daucyl ^[f]	epi	<i>Mc</i> -FCC-56	[28a]
epi-42	OH	CH ₃	4'-daucyl ^[g]	epi	<i>Mc</i> -FCC-53	[28a, 85]
25	OH	CH ₃	^[h]	n	<i>Sw</i> -FCC-62	[74]
epi-25	OH	CH ₃	^[h]	epi	<i>Ma</i> -FCC-69	[76]
epi-26	OH	CH ₃	^[i]	epi	<i>Ma</i> -FCC-61	[28b]
epi-27	OH	CH ₃	^[j]	epi	<i>Ma</i> -FCC-63	[76]
epi-28	OH	CH ₃	^[k]	epi	<i>Ma</i> -FCC-64	[76]
epi-43	O-Glc ^[d]	CH ₃	5'-daucyl ^[f]	epi	<i>Mc</i> -FCC-49	[85]
epi-44	O-Glc ^[d]	CH ₃	4'-daucyl ^[g]	epi	<i>Mc</i> -FCC-46	[85]
45	O-Glc ^[d]	CH ₃	H	n	<i>At</i> _{MES} -FCC	[67]
34	OH	H	H	n	<i>At</i> -DFCC-33	[26c]
35	OH	CH ₃	H	n		[27]
40	H	CH ₃	H	n	<i>At</i> _{MES} -2HM- <i>iso</i> -DFCC	[26a]

[a] Compound numbering (see text), R³ = vinyl. [b] Relative configuration at C16: n = normal, that is, derived from *p*FCC, or epi = epimeric, that is, derived from *epi-p*FCC. [c] *Bn*-FCC-2 (from oilseed rape, *B. napus*),^[25] *Ca*-FCC-2 (from sweet pepper, *C. annuum*),^[47] *At*-FCCs (from *A. thaliana*),^[60] *Mc*-FCCs (from banana peels),^[28a, 51] *Ma*-FCCs (from banana leaves, *M. acuminata*, Cavendish cultivar),^[28b, 76] and *Sw*-FCC-62 (from senescent leaves of *S. wallisii*).^[74] [d] Glc = β -glucopyranosyl. [e] Apparently an artefact from the methanolysis of persistent FCC daucyl esters. [f] Daucic acid bound at 5'-OH. [g] Daucic acid bound at 4'-OH. [h] R⁴ = 6- β -glucopyranosyl-(1-1')-2-[3,4-dihydroxyphenyl]ethyl. [i] R⁴ = 6- α -galactopyranosyl-(1-6)- β -galactopyranosyl-(1-1)-glyceryl. [j] R⁴ = 6- β -glucopyranosyl. [k] R⁴ = 6- α -glucopyranosyl.

of the methyl ester function of 3²-hydroxy-*p*FCC (**23**) and of *p*FCC (**6**), respectively (Table 2).^[60]

The actual in vivo presence of (other) modified FCCs with a free propionic acid function has rarely been documented. Therefore, the intermediate natural existence of other *m*FCCs has, so far, been deduced from structure determination of the various natural NCCs, the presumed direct isomerization products of correspondingly modified *m*FCCs (Figure 15).^[6b, 9c, 10] The NCC structures suggest a range of corresponding FCC modifications that are probably (or are known to be) introduced by cytosolic enzymes.^[9c] Interestingly, the unique modification of *At*-NCC-3 (**15**) at C2 indicated a divergent catabolic process in *A. thaliana*,^[66] which was rationalized by a side chain hydroxylation of *p*FCC (**6**) lacking exclusive selectivity for C3².

In contrast to the fleeting existence of typical FCCs, a strikingly persistent and remarkably abundant FCC (> 13 %

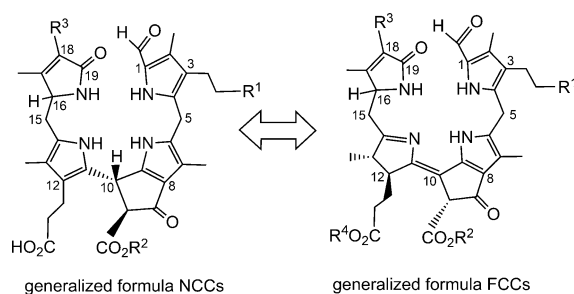


Figure 15. Structures of hypothetical modified FCCs (*m*FCCs, right) are frequently extrapolated from those of the corresponding isomeric NCCs (left).

the ester functions of digalactosyldiacylglycerols with loss of the polar head group.^[75] A small additional group of less-polar *hm*FCCs from the banana leaves was identified subsequently

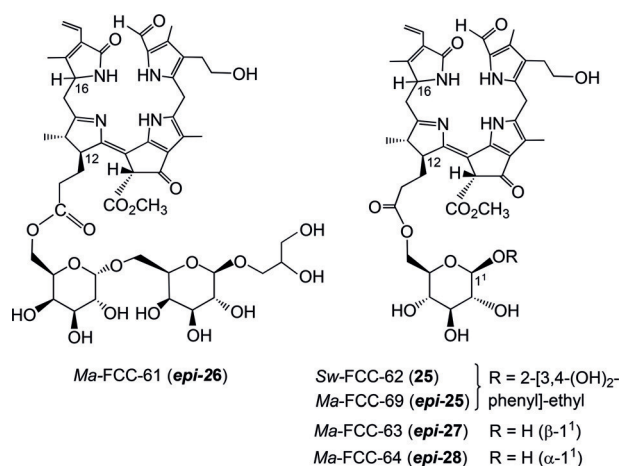


Figure 16. Top: Structural formulas of *hm*FCCs from leaves of bananas (*Ma*-FCCs) and of *Sp. wallisii* (*Sw*-FCC-62), and reproduction (bottom) of a cover picture depicting a yellow banana leaf when observed under daylight or under black light.^[28b]

and turned out to represent FCC esters with β -glucopyranosyl units attached at the critical propionate at O6' (their primary OH group). Among these *hm*FCCs, *Ma*-FCC-69 featured a 3,4-dihydroxyphenylethyl aglycon at its glucopyranosyl ester moiety, thus representing the C16 epimer (*epi-25*)^[76] of *Sw*-FCC-62 (**25**) from leaves of *Sp. wallisii*.^[74] This normal/epi stereodivergence is due to the differing classes of RCC reductases: in banana leaves (and, likewise, in banana fruit; see Section 6), a reductase of the RCCR-2 type is present, whereas in *Sp. wallisii*, an RCCR-1 produces colorless Chl catabolites of the normal series.^[74]

FCCs accumulate in a striking abundance in senescent banana leaves, but NCCs were not detected, nor was there any indication of the presence of type-II phyllobilins.^[76] In the two less-polar *hm*FCCs from banana leaves, *Ma*-FCC-63 (*epi-27*) and *Ma*-FCC-64 (*epi-28*), a β - or an α -glucopyranosyl moiety, respectively, was attached through the primary 6'-OH group. The free anomeric center of *epi-27* and *epi-28* allowed for the mutual interconversion by spontaneous anomerization in aqueous solution.^[76] The presence of the latter anomeric *hm*FCCs, *epi-27* and *epi-28*, in extracts of senescent banana leaves strengthened the suggestion that the observed

*hm*FCCs could either be precursors, or, possibly, remnants or partial degradation products of still elusive further functionalized *hm*FCCs. Esterification of the critical propionate function of FCCs by glucopyranosyl or, alternatively, by galactopyranosyl groups provides two distinct lines among the persistent banana leaf *Ma*-FCCs. The sugar units of these *hm*FCCs provide attachment sites for further groups. Indeed, several minor, still less polar FCC fractions were recently analyzed structurally, and were revealed to be *hm*FCCs, formally derived from *epi-27/epi-28*, but functionalized further by unusual terpenoid aglycons with β -glycosidic linkages.^[77]

4.2. The Type-II Phyllobilin Branch—Colorless 1,19-Dioxobilins

The discovery of 1,19-dioxobilin-type NCCs (DNCCs) raised the question of their formation and of their natural relevance in Chl breakdown.^[57,58] As products of the PaO/phyllobilin pathway, the native phyllobilins are 1-formyl-19-oxobilins (or type-I phyllobilins).^[9c,10] DNCCs, the 1,19-dioxobilin-type Chl catabolites, are the offspring of a subsequent step of Chl breakdown and are, thus, classified as type-II phyllobilins. Interestingly, the 1,19-dioxobilin-type structure of DNCCs (Figures 11 and 17)^[57,58] makes them look

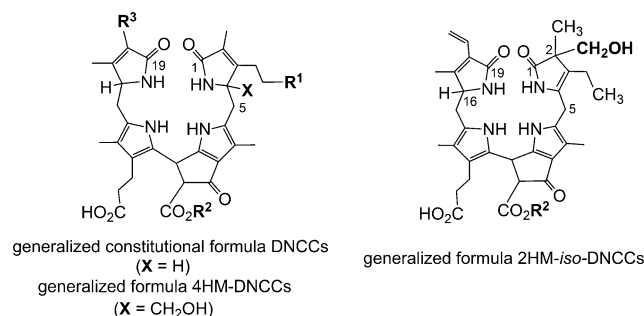


Figure 17. Generalized formulas of colorless and nonfluorescent type-II phyllobilins: DNCCs, 4-hydroxymethyl-DNCCs and 2-hydroxymethyl-iso-DNCCs.^[26]

remarkably similar to the heme-derived bilins, the hemobilins.^[3] Recent studies have revealed a striking abundance and constitutional and stereochemical variety of DNCCs that rivals that of the now better studied NCCs, and populating a growing second branch of phyllobilins, of the type-II phyllobilins.^[10]

1,19-Dioxobilin-type nonfluorescent Chl catabolites (DNCCs) are formal products from an oxidative removal of the formyl group of NCCs.^[57] The lack of the characteristic absorption of NCCs at $\lambda \approx 315$ nm (Figure 9) makes DNCCs more difficult to detect by their UV absorption. Such colorless dioxobilin-type Chl catabolites (DCCs) accumulate in a variety of senescent leaves. DCCs may occur in leaves together with type-I phyllobilanes, as is the case in senescent leaves of *A. thaliana*. In wild-type *A. thaliana* leaves, the polar 1,19-dioxophyllobilane *At*-DNCC-33 (**30**) is, by far, the most abundant phyllobilin, with isomeric *At*-DNCC-45 (**31a**) and

Table 3: Structures of natural dioxobilane-type nonfluorescent Chl catabolites (DNCCs, top section) and of *iso*-DNCCs (bottom section): labels R¹, R², and R³ refer to the general constitutional formula of DNCCs and *iso*-DNCCs, shown in Figure 17.

No. ^[a]	R ¹	R ²	R ³	C16 ^[b]	Provisional names ^[c]	Ref.
31 a/31 b	H	H	CH=CH ₂	n	<i>At</i> -DNCC-45/ <i>At</i> -DNCC-48	[26c]
32	H	CH ₃	CH=CH ₂	n	<i>At</i> _{MES} -DNCC-47	[26a]
33	OH	CH ₃	CH=CH ₂	n	<i>At</i> _{MES} -DNCC-38	[26a]
<i>epi</i>-33	OH	CH ₃	CH=CH ₂	<i>epi</i>	UNCC- <i>Pvir/Vv</i> -DNCC-51	[78]
30	OH	H	CH=CH ₂	n	<i>At</i> -DNCC-33/ <i>Bo</i> -DNCC-3	[27, 61]
8 a	OH	CH ₃	CH(OH)-CH ₂ OH	n	–	[57]
8 b	OH	CH ₃	CH(OH)-CH ₂ OH	n	–	[57]
<i>ent</i>-8 a	OH	CH ₃	CH(OH)-CH ₂ OH	<i>epi</i>	<i>Ap</i> -DNCC	[58]
36	H	H	CH=CH ₂	n	<i>At</i> -2HM- <i>iso</i> -DNCC-43 ^[d]	[26b]
37	H	H	CH=CH ₂	n	<i>At</i> -4HM-DNCC-41 ^[e]	[26b]
38	H	CH ₃	CH=CH ₂	n	<i>At</i> _{MES} -2HM- <i>iso</i> -DNCC-46 ^[c]	[26a]
39	H	CH ₃	CH=CH ₂	n	<i>At</i> _{MES} -4HM-DNCC-44 ^[d]	[26a]

[a] Compound number (see text). [b] Configuration at C16: n = normal, if derived from *p*FCC, or *epi* = epimeric, if derived from *epi-p*FCC; configuration at C4 not determined. [c] *Ap*-DNCC (from *Acer platanoides*);^[58] *At*-DNCCs (from *A. thaliana*, wild type)^[26b] or *At*_{MES}-DNCCs (from *A. thaliana*, MES16 mutant).^[26a] [d] Hydroxymethyl group at C2; UNCC-*Pvir/Vv*-DNCC-51 (from grape wine).^[78] [e] Hydroxymethyl group at C4 (see Figure 17 for generalized formulas of DNCCs and *iso*-DNCCs).

At-DNCC-48 (**31 b**) being minor components.^[27] The 1,19-dioxophyllobilanes *At*_{MES}-DNCC-47 (**32**) and *At*_{MES}-DNCC-38 (**33**) were found in extracts of the *A. thaliana* MES16 mutant (besides minor NCC fractions; Table 3).^[26a] Bilane **33** is a C16 epimer of *Vv*-DNCC-51 (*epi*-**33**) from degreened grape wine leaves.^[78] The isomeric DNCCs **8 a**, **8 b**, and *ent*-**8 a** (Figure 10 and Table 3) were discovered in senescent leaves of barley^[57] and of Norway maple.^[58]

The observation of 1,19-dioxobilin-type NCCs (DNCCs) first raised the question of their formation and of their general metabolic relevance for natural Chl breakdown.^[57,58] Based on a stereochemical divergence indicated by the deduced structure of the DNCC *ent*-**8 a** from leaves of Norway maple, a split of the PaO/phyllobilin pathway at the level of the fluorescent Chl catabolites (FCCs) was proposed, which, in consequence, would involve the intermediate existence of one (or of several) 1,19-dioxobilin-type fluorescent Chl catabolite (or DFCC) intermediate(s).^[58]

Indeed, a cytochrome P450 enzyme (CYP89A9) was recently identified in *A. thaliana* that catalyzed the *in vitro* deformylation of *epi-p*FCC (*epi*-**6**), thereby furnishing four epimeric DFCCs.^[27] A pair of these DFCC epimers isomerized rapidly to a pair of DNCCs in weakly acidic solution. These *in vitro* experiments clarified the basic constitutional features of an FCC deformylation and of the DFCC to DNCC isomerization, proposed to be early key steps of the dioxobilin branch of Chl breakdown.^[27] Clearly, the intriguing deformylation by the cytochrome CYP89A9 requires further investigation. General precedence for the removal of formyl (or acyl) groups by P450 enzymes exists.^[79] However, there appears to be none for a P450-catalyzed

oxidative deformylation at an α -position of a pyrrole unit. The inferred nucleophilic (hydro)peroxy-Fe^{III} intermediate of the P450 cycle was suggested to induce oxidative (C–C) bond cleavages.^[79b,80] This would thus imply an insertion of oxygen atom into the previous (C–C) bond with formation of a formate ester, reminiscent of the Baeyer–Villiger reaction (Figure 18, bottom). Hydrolysis of this putative ester, removal of the currently unknown C1 fragment (possibly formic acid), and protonation at C4 could all take place without assistance by the P450 enzyme, thereby helping to explain the lack of stereoselectivity observed in the *in vitro* experiment with CYP89A9.^[27]

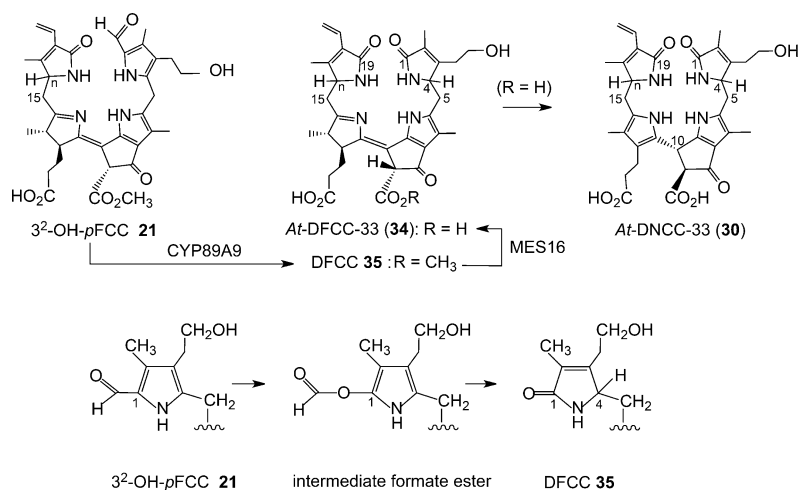


Figure 18. Top: Deformylation of 3²-OH-*p*FCC by CYP89A9 is proposed as an entry to type-II phyllobilins by furnishing the hypothetical DFCC 35; ester hydrolysis by MES16 produces DFCC 34 (*At*-DFCC-33), which isomerizes to DNCC 30 (*At*-DNCC-33).^[26c] Bottom: Abridged outline of a possible mechanism (depicted by ring A) of the deformylation of FCC 21 to DFCC 35, catalyzed by the cytochrome P450 enzyme CYP89A9.^[26a]

Thus, the remarkable *in vitro* results with CYP89A9 did not provide a firm conclusion with respect to the stereochemical outcome of the DFCC/DNCC isomerization, nor was a major step of the natural dioxobilin pathway clearly identified. Careful analysis of an extract of *A. thaliana* leaves at an early degreening stage, revealed a minor (blue) fluorescent fraction exhibiting a characteristic band at $\lambda = 360$ nm (from the conjugated B/C part corresponding to FCCs), but lacking the absorption at $\lambda = 320$ nm of an α -formylpyrrole unit (Figure 8). A sample of the fleetingly existent natural DFCC 34 (a 3²-hydroxy-1,4,12,13,16,19-hexahydro-1,19-dioxophyllobilene-*b*) was recently isola-

ted.^[26c] The structure of **34** was deduced from mass spectrometric and extensive NMR-spectroscopic analysis.^[26c] The DFCC **34** readily underwent acid-induced, stereoselective isomerization at pH 5 to generate a single DNCC (Figure 18). The isomerization product was identified as *At*-DNCC-33 (**30**),^[26c] the major natural DNCC in senescent leaves of *A. thaliana*.^[27] The DFCC **34** was proposed to be the hydrolysis product of the corresponding, still elusive, methyl ester (DFCC **35**), generated by CYP89A9-catalyzed deformylation of 3²-OH-*p*FCC (**23**).^[26c] Hence, a naturally existing, functionalized DFCC was identified and, simultaneously, an important natural branching point to the type-II phyllobilins was revealed in a higher plant.

5. Chl Breakdown in *Arabidopsis thaliana*—A Model Case

The growing systematic biological knowledge concerning *Arabidopsis thaliana* has also become an important resource in the field of Chl breakdown,^[27] assisting the identification of a number of enzymes in this model plant,^[9c,11a] in fruitful synergy with our recent complementary work concerned with the discovery and structure elucidation of an extraordinary number of Chl catabolites.^[26,27,60,67] A range of colorless type-I phyllobilins were found in earlier analyses of extracts of senescent leaves of (wild-type) *A. thaliana*, including five *At*-NCCs (**3**, **4**, **15–17**),^[60,66] see Table 1) and three *At*-FCCs (**6**, **22**, **24**, Table 2).^[60] More recently, colorless type-II phyllobilins were discovered in *A. thaliana*, and the *At*-DNCCs **30**, **31a**, and **31b** were characterized (Table 3),^[26b,27] as well as the fleetingly existent DFCC **34**.^[26c]

However, various further colorless, nonfluorescent phyllobilins were observed, apparently related to DNCCs, in extracts of senescent leaves of *A. thaliana* (either of wild type^[26b] or of the MES16 mutant^[26a]). These were, provisionally, classified as nonfluorescent DCCs (NDCCs) on the basis of their UV spectra, which were similar to those of the structurally characterized 1,19-dioxobilin-type NCCs (DNCCs) **30** and **31a/31b**. However, as deduced from mass spectra and NMR-spectroscopic analyses, several of these NDCCs exhibited a puzzling carbon-hydroxymethylation and, thus, did not have the proper chemical constitution of DNCCs.^[26a,b] A 2-hydroxymethyl-*iso*-DNCC (*At*-2HM-*iso*-DNCC-43, **36**) and a 4-hydroxymethyl-DNCC (*At*-4HM-DNCC-41, **37**) were discovered (Figure 19 and Table 3)^[26b]

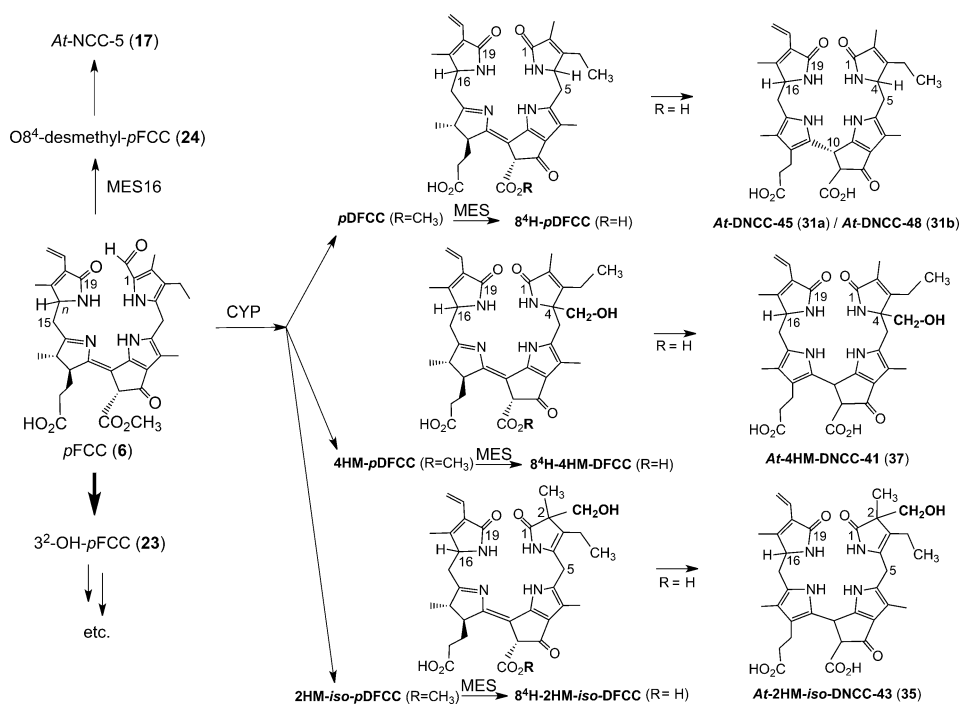


Figure 19. Phyllobilins lacking a 3²-OH group are directly derived from *p*FCC (**6**). In vivo deformylation of *p*FCC(**6**) in *A. thaliana* by CYP89A9 (CYP) and hydrolysis by the methyl esterase MES16 (MES) is a pathway to three types of nonfluorescent DCCs (right: the genuine DNCCs **31a/31b**, 2HM-*iso*-DNCC **35**, 4HM-DNCC **37**), proposed to be formed by isomerization of the corresponding hypothetical fluorescent DCCs with R = H (center: 8⁴H-*p*DFCC, 8⁴H-2HM-*iso*-DFCC, and 8⁴H-4HM-DFCC).^[26b]

in extracts of senescent leaves of wild-type *A. thaliana*, while the corresponding methyl esters 2-hydroxymethyl-*iso*-DNCC *At*_{MES}-2HM-*iso*-DNCC-46 (**38**) and the 4-hydroxymethyl-DNCC *At*_{MES}-4HM-DNCC-44 (**39**) were found in extracts of the MES16-mutant of *A. thaliana*.^[26a] In the leaves of this mutant, an additional minor fraction of a colorless blue fluorescent phyllobilin was noticed, which lacked the $\lambda = 315$ nm band in the UV spectra, but showed the characteristic absorption maximum of FCCs near $\lambda = 360$ nm.^[26a] Thus, this fluorescent compound was tentatively classified as a fluorescent DCC (FDCC). It was isolated and characterized as the 2-hydroxymethyl-*iso*-DFCC *At*_{MES}-2HM-*iso*-DFCC (**40** = 2HM-*iso*-*p*DFCC, see Figure 19),^[26a] which differed from genuine DFCCs by the constitution of its ring A (Figure 19 >). The structural properties of the FDCC **40** suggest its role as the direct precursor of the *At*_{MES}-2HM-*iso*-DNCC-46 (**38**),^[26a] its nonfluorescent isomer. All of these remarkable carbon-hydroxymethylated type-II phyllobilins lack an oxygen functionality at their C3²-position, which is typical of most natural phyllobilins.^[9c,10] Hence, their structures relate them to *p*FCC (**6**) as their (direct) precursor. Hydroxymethylation appears to be tightly associated with the oxidative deformylation of *p*FCC to type-II products. Possibly, it is a cytosolic “rescue operation” that introduces a (needed) polar functionality at ring A of the catabolites. In this sense, the hydroxymethylation (at the carbon atom) has been considered a “biosynthetic intermezzo” in the course of the type-II branch of the PaO/phyllobilin pathway.^[26a,b]

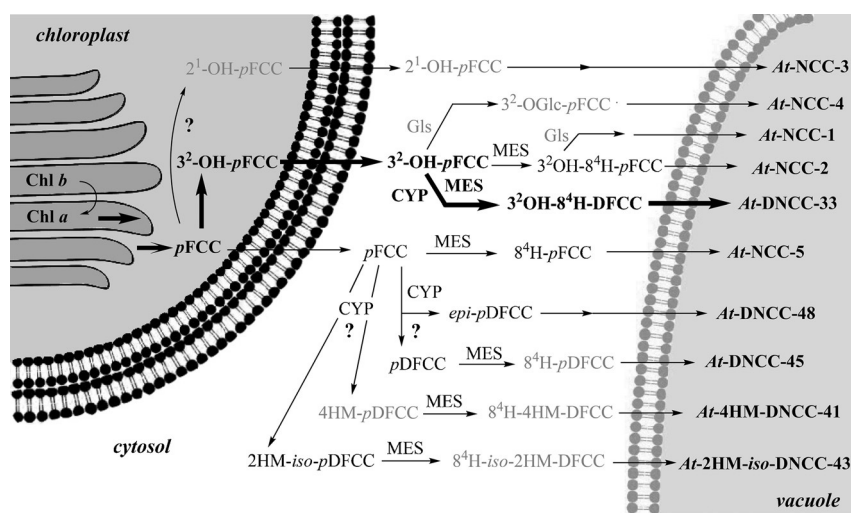


Figure 20. Overview of Chl breakdown in leaves of *A. thaliana* (wild type). The proposed major pathway, from Chl *a* to At-DNCC-33,^[26c] is marked with bold arrows (CYP = CYP89A9, MES = MES16, Gls = putative glycosidase; see Figure 19 for the structures of type-II phyllobilins derived from pFCC).

In summary, a vast variety of colorless phyllobilins are produced in *A. thaliana* by breakdown of Chl, spearheaded by formation of pFCC (6) in the chloroplasts, as well as, presumably, of 3²-hydroxy-pFCC (23).^[9c,26c] The descendants of pFCC (6) that lack an OH group at the C3²-position are minor components among the Chl catabolites in *A. thaliana*, despite their particularly diverse nature (Figures 19 and 20). The major phyllobilins in *A. thaliana* (both the wild type and MES16 mutant) are, instead, derivatives of 3²-hydroxy-pFCC (23). Its type-II phyllobilin descendants dominate over the type-I analogues. Evidence for export of the FCCs 6 and 23 into the cytosol and for their further independent processing to modified FCCs, DFCCs, and FDCCs is derived from the structures of the FCCs 22, 24, DFCC 34, and FDCC 40, as well as of their nonfluorescent descendants. The latter are believed to arise by acid-catalyzed isomerization of their fluorescent precursors after import into the vacuoles. The deduced *in vivo* deformylations of pFCC (6) and of 3²-hydroxy-pFCC (23) establish two natural branching points from type-I to type-II phyllobilins in leaves of *A. thaliana*.^[26c]

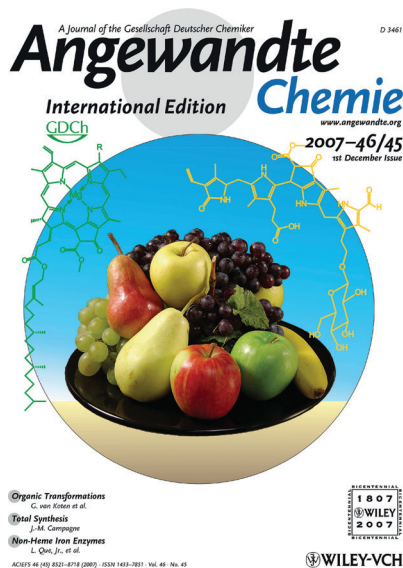


Figure 21. Ripening fruit (left) and degreening florets of broccoli (right) undergo Chl breakdown and accumulate colorless phyllobilins.^[59,61]

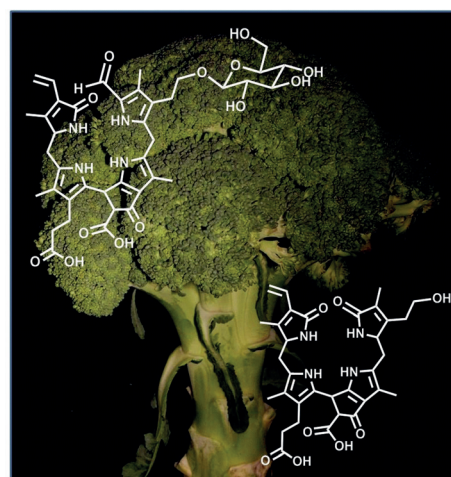
6. Long Overlooked Chl Catabolites in Fruit and Vegetables

The disappearance of chlorophyll is commonly associated with the appearance of fall colors. However, ripening fruit (and also vegetables) often undergo degreening processes (Chl breakdown) that are visually similar to those observed in senescent leaves (Figure 21).^[9c,11c] Hence, the question arose “What happens to Chl when fruit ripen and vegetables degreen?”

6.1. Colorless Chl Catabolites in Fruit and Vegetables

As a rule, when apples, pears, or other fruit ripen, the associated appearance of the appetizing colors of the ripe fruit is a visual indicator of their degree of ripeness.^[81] At the same time, the Chl originally present in the unripe green fruits is

broken down, presumably to produce phyllobilins. Chl breakdown in the peel of Golden Delicious apples (*Malus domestica*) and of Williams pears (*Pyrus communis*) was shown to yield the nonfluorescent type-I phyllobilins *epi-9* and *epi-11*, also named *Md-NCCs* and *Pc-NCCs*.^[59] The same (*epi*-type, that is, RCCR-2 derived) NCCs were also found in senescent leaves of the corresponding apple and pear trees, thereby indicating a common pathway in the leaves and fruit of these fruit trees.^[59] Several NCCs, including *Ej-NCC-2* (*epi-29*, Table 1), were identified (on the basis of mass-spectrometric and UV-spectroscopic data) in quince (*Cydonia oblonga*, Miller)^[82] and in loquat fruit (*Eriobotrya japonica*).^[83] Likewise, the NCCs *Bo-NCC-1* (3) and *Bo-NCC-2*



(17), as well as *Bo*-DNCC-3 (30), were characterized in degreening broccoli florets (*Brassica oleracea*, var. Ital.). These three NCCs are known representatives of the normal stereochemical series of type-I and type-II phyllobilins.^[61] Five NCCs were described earlier in senescent spinach leaves (*Spinacia oleracea*), the so-called *So*-NCCs (*epi*-1, *epi*-5, *epi*-11, *epi*-12, *epi*-13), which belong to the *epi* series of NCCs.^[50,64] As expected, in ripe(ning) fruit and (degreening) vegetables, Chl breakdown follows the common PaO/phytyllobilin pathway and furnishes colorless type-I and type-II phyllobilins, in a species-dependent way. Clearly, these plant-derived components of our food are a common source of Chl catabolites, which, hence, are part of our daily nutrition.^[6a]

6.2. Persistent Blue Luminescent Chl Catabolites in Bananas

The ripening of bananas is associated with the typical development of a bright yellow color, which, in turn, is commonly considered a critical visual indicator of the degree of ripeness of the banana fruit. Clearly, during the degreening process, the Chl present in the peels of the unripe fruit is degraded. We were, therefore, intrigued to analyze bananas for Chl catabolites.^[28a] Surprisingly, some of the catabolites found in the peels of freshly ripe bananas (*Musa acuminata*, Cavendish cultivar) were revealed to be persistent FCCs and to belong to the then unprecedented group of hypermodified FCCs (*hm*FCCs). These FCCs make the ripening bananas glow blue, as is best seen when analyzed by irradiation with black light and observation in a dark room (Figure 22).^[28a] Several persistent *hm*FCCs accumulate in the peels of ripe(ning) bananas, where the *Mc*-FCCs *epi*-23, *epi*-41, and

epi-42 represent a sizeable fraction of the phyllobilins. The major *hm*FCCs of the peel of ripe bananas, *Mc*-FCC-56 (*epi*-41) and *Mc*-FCC-53 (*epi*-42), feature an ester at the propionic acid function that is derived from daucic acid^[84] itself.^[28a] The more polar *Mc*-FCC-49 (*epi*-43) and *Mc*-FCC-46 (*epi*-44) are further modified at their 3²-positions by a β -glucopyranosyl unit (Table 2 and Figure 22).^[28a,85] Thus, *Mc*-FCCs differ characteristically from related *hm*FCCs so far found in senescent leaves of bananas^[51] or of the Peace Lily,^[74] which are all esterified with typical natural hexopyranosyl units.

In the early phase of the ripening process of bananas, the classical FCC 3²-hydroxy-*epi*-*p*FCC (*Mc*-FCC-62, *epi*-23) could also be observed as a major FCC fraction, the rational precursor of the hypermodified FCCs (*hm*FCCs) in the banana peel.^[51] In addition, a variety of *Mc*-NCCs were characterized in extracts of the banana peels. However, similar to the banana leaves,^[76] representatives of the type-II phyllobilins were not detected.^[51] These findings indicated an exclusive role of type-I phyllobilins (of the *epi*-type) in banana peels, as well as a pathway of Chl breakdown that diverges into two branches of type-I phyllobilins at the level of FCCs (Figure 23). This stage of Chl breakdown is presumed to be located in the cytosol, where formation of specific *hm*FCCs through esterification of 3²-hydroxy-*epi*-*p*FCC (*epi*-23) with a daucyl group competes with other modifications that furnish typical *m*FCCs. The latter are presumed to be transported into the vacuoles for eventual rapid isomerization to *Mc*-NCCs (Table 1).^[51]

As is commonly observed, dark, senescence-associated spots develop naturally on the peels of very ripe bananas.^[87] This deterioration can be inhibited by protection from air (or oxygen).^[88] These spots arise around the stomata as a sign of local senescence and eventual cell death.^[85] Strangely, glucosylated *hm*FCCs (especially *epi*-43 and *epi*-44) accumulate specifically in the senescent area around the dark spots. This local FCC enrichment in areas encircling the growing necrotic spots can easily be observed in darkened rooms, when black light is used as the light source.^[85] The blue fluorescent rings observed on the peels of overripe bananas arise in areas committed to programmed cell death, and have, thus, been considered to represent “blue halos of cell death”.^[85]

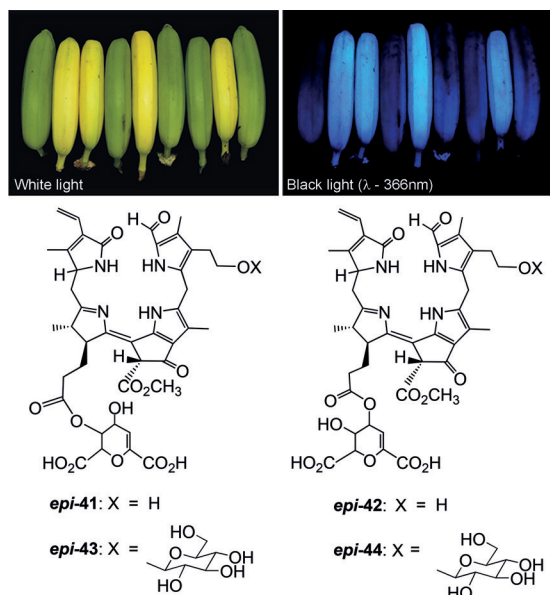


Figure 22. Top: Yellow ripe bananas show a blue luminescence. When yellow bananas are illuminated with UV light (black light), a blue glow of the bananas originates from the abundant FCCs and can be seen by the naked eye^[86] (picture taken from Ref. [28a]). Bottom: Major *hm*FCCs from banana peels are FCC daucyl esters.^[28a,85]

7. Phyllochromobilins from Oxidation of Phylloleucobilins

Early on, NCCs were called “rusty pigments”.^[8a,14] Indeed, samples of these colorless products of Chl catabolism, which often accumulate as apparently final products of Chl breakdown in senescent leaves of higher plants, readily become rust colored.^[7] Analysis of such a colored mixture obtained by exposure of a solution of the common NCC *epi*-11 to sunlight in the presence of air revealed the presence of the yellow compounds 46Z and 46E, as well as of pink-colored 47, which we classified as yellow Chl catabolites (YCCs) and pink Chl catabolites (PiCCs), respectively (Figure 24).^[6b,7,89]

YCC **46Z** from **11** or *epi-11*, as well as from some other NCCs.^[91] The scope of this type of “green synthesis with leaves” on the basis of their still puzzling oxidative activity remains to be explored, as does the selectivity and preparative limitations of this type of transformation. An analogous oxidation with DNCCs (as observed with NCCs **11** and *epi-11*^[91]), could provide a possible pathway to the corresponding dioxobilin-type YCCs (DYCCs). YCC-type compounds were not only detected in senescent leaves of *C. japonicum*,^[7] but also in fresh extracts of a variety of senescent leaves, for example, of the deciduous lime^[92] and *Egeria densa* trees,^[93] as well as in the peel of ripe bananas.^[51]

7.2. Pink Phyllobilins—The Phylloroseobilins

Similar to bilirubin (BR),^[90] YCCs are easily oxidized in the presence of air or molecular oxygen. Pink Chl catabolites, classified as PiCCs, are obtained from the oxidation of YCCs.^[89] For synthetic purposes, the oxidation of, for example, the YCC **46Z**, can be achieved efficiently in the presence of an excess of Zn^{II} ions, thereby furnishing the bright blue Zn^{II} complex **Zn-47**.^[94] Treatment of **Zn-47** with

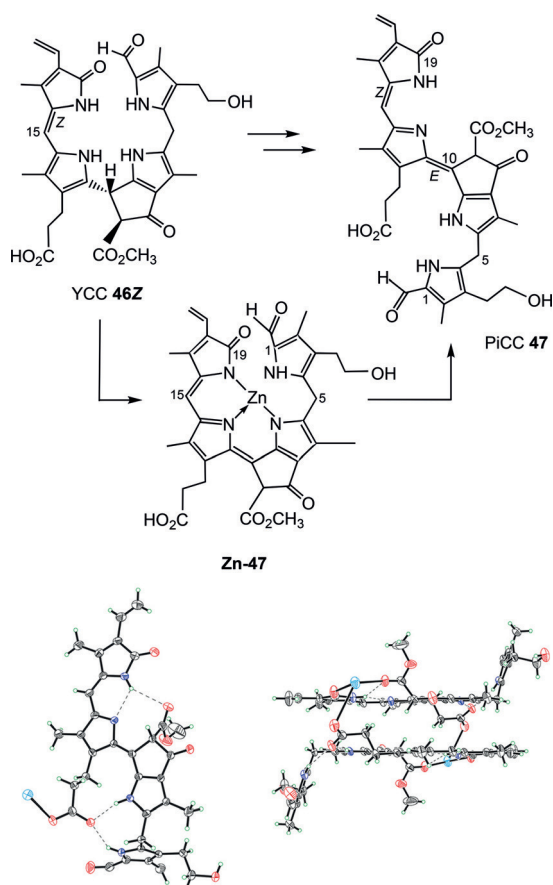


Figure 26. Top: Oxidation of YCC **46Z** in the presence of Zn^{II} ions furnishes the blue Zn^{II} complex **Zn-47**, from which the PiCC **47** is liberated by treatment with acid or phosphate; bottom: molecular structure of the PiCC **47** as deduced from X-ray crystal structure analysis (C gray, green H, red O, blue N; left: top view, right: side view).^[94a]

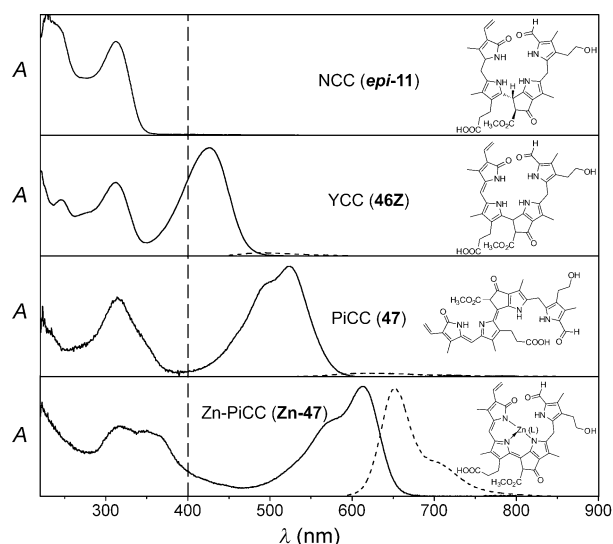


Figure 27. UV/Vis spectra (—, left axis) and fluorescence emission spectra (---, right axis) of NCC *epi-11* (top) and of the phyllochromobilins **46Z** (a YCC) and **47** (a PiCC), as well as of the blue Zn^{II} complex **Zn-47**.^[94]

acetic acid or phosphate removes the Zn ion and liberates the PiCC **47** nearly quantitatively (Figure 26).^[94a] The pink phyllobiladiene-*b,c* **47** features a long-wavelength absorption band at $\lambda \approx 520$ nm, consistent with the further extension of the conjugated π system to ring B (Figure 27). The chromophore of the PiCC **47** exhibits a remarkable correspondence to that of the heme-derived bilin phycoviolobin.^[3,56] Desaturation of the “southern” C10-position of the YCC **46Z** caused the PiCC **47** to become available as a racemate: its single asymmetric center (C8²) is acidified by adjacent functionalities that assist its fast racemization.^[94a] Detailed NMR-spectroscopic analysis of the PiCC **47** indicated a striking *E* configuration of the C10=C11 double bond. An X-ray crystal-structure analysis confirmed the NMR-derived structure and revealed the oxidized phyllobiladiene-*b,c* **47** as a pair of hydrogen-bonded enantiomers in the crystal, which π stack, thanks to their extended planar chromophore system (see Figure 26).^[94]

The recent observations of the natural occurrence of YCCs and PiCCs points to a more general relevance of further endogenous transformations of colorless Chl catabolites in senescent plants that go beyond the stage of the abundant type-I and type-II phylloleucobilins. Such endogenous processes may represent important further steps of natural Chl breakdown, thereby helping to explain the eventual pronounced decrease in the amount of colorless phyllobilin-type Chl catabolites in leaves, frequently noted when analyzing leaves undergoing progressive senescence over several days to weeks.

8. Phyllobilins Are Natural Products with Remarkable Properties

Phyllobilins, Chl-derived linear tetrapyrroles,^[10] have structures related to those of the heme-derived (hemo-)bilins.^[3,90] Accordingly, phyllobilins are expected to display diverse photo-, coordination and redox chemistry. However, the chemical properties of phyllobilins have barely been explored to date.^[10,94b,95]

8.1. Phyllobilins as Photoactive Tetrapyrroles

The photochemical properties of the breakdown products of the green photosynthetic pigment Chl have been of prime interest. The observed rapid catabolic transformation of Chl into colorless phyllobilins has been rationalized primarily as the destruction of potentially phototoxic Chl. Hence, the observed rapid formation of the nonfluorescent and colorless type-I and type-II phyllobilins (NCCs and DNCCs) is completely in line with such a detoxification aspect of Chl breakdown. Indeed, NCCs and DNCCs, which typically accumulate in senescent leaves, display absorptions limited to the UV region of sunlight (Figure 8), and they, furthermore, lack photoactivity.

Remarkably, photoactive breakdown intermediates do not typically accumulate during the rapid breakdown of Chl on the way to the nonfluorescent phyllobilins. Fluorescent Chl catabolites, such as *p*FCC (**6**) and 3²-hydroxy-*p*FCC (**23**), as well as their C16 epimers, represent an important intermediate stage in the PaO/phyllobilin pathway.^[9c] The FCC **6** absorbs very little light in the visible region (Figure 9). As their classification suggests, FCCs are effective emitters of blue fluorescence.^[28a,95] Thus, *epi-23-Me*, the semisynthetic methyl ester of 3²-hydroxy-*epi-p*FCC (*epi-23*) features an emission with a maximum at $\lambda = 437$ nm and a fluorescence quantum yield of 0.21 (lifetime: 1.6 ns in ethanol).^[95] The photoexcited *epi-23-Me* undergoes intersystem crossing into the triplet state (with a quantum yield of 0.6), from which it generates singlet oxygen with nearly 100% efficiency. Thus, the FCC *epi-23-Me* is a remarkably potent sensitizer of singlet oxygen (¹O₂). However, FCCs exist only fleetingly in senescent leaves, except when “caged” as the persistent hypermodified FCCs (*hm*FCCs).^[28a] The deduced, similar photochemical features of *hm*FCCs are noteworthy, as they may play a physiological role in senescent plant tissue and in ripening fruit (see Section 9).

Colorless NCCs are transformed into the yellow YCCs (e.g. **11** into **46Z**) by desaturation at their C15-position. Similar to their distant analogue BR,^[90] YCCs absorb blue light (absorption maxima at $\lambda \approx 430$ –440 nm) and exhibit only a weak emission with a maximum at $\lambda \approx 500$ nm (Figure 27), which indicates rapid deactivation of their excited states.^[94b] Similar to BR, the YCC **46Z** undergoes light-induced *E/Z* isomerization to **46E**.^[89] Oxidation and desaturation of **46Z** at the C10-position produces the PiCC **47**, which absorbs at $\lambda \approx 520$ nm, and emits weakly (with a maximum at $\lambda \approx 620$ nm, Figure 27).^[94a]

8.2. Phyllobilins as Antioxidants

As is typical for bilanes and strongly reduced hydro-porphinoids,^[96] NCCs are easily oxidized.^[89] In line with this property, they are also remarkable amphiphilic antioxidants,^[59] as evident by their inhibitory effect in the classical autoxidation reaction of linoleic acid.^[97] In such tests, the NCC *epi-11* exhibited an only five times lower capacity than bilirubin (BR),^[59] an effective and physiologically important antioxidant.^[97] Analogous investigations of the effect of the corresponding YCC **46Z** on the autoxidation of linoleic acid indicated this YCC to even inhibit about 3–5 times more effectively than BR, not unexpected in view of the similar features of their chromophores.^[98] Experiences on the antioxidant effect of other phyllobilins (such as model FCCs, DNCCs, and DYCCs) would also be of interest. This aspect of the properties of phyllobilins still remains to be studied.

8.3. Phyllobilins as Ligands in Transition-Metal Complexes

In contrast to the cyclic tetrapyrroles, which enrich nature with the important metalloporphyrinoid cofactors,^[71,99] a less typical feature of linear tetrapyrroles is their ability to bind metal ions.^[3,100] However, heme-derived bilins and phyllo-(chromo)bilins can be considered to share similar features as multidentate ligands for (transition-) metal ions.^[94b,100] Four nitrogen centers are available in linear tetrapyrroles for the coordination of metal ions.^[94b] However, N atoms of isolated pyrrole rings can hardly compete with polar solvent molecules for coordination at metal ions. Therefore, the photoinactive nonfluorescent NCCs and DNCCs are judged as lacking the capacity for complexing.^[94b] In contrast, the availability of nitrogen atoms of the imine and enamine types in phyllochromobilins provides centers for coordination to transition-metal ions. So far, the scarcity of such phyllobilins has limited the corresponding studies to the coordination behavior of PiCC **47** and, to some extent, of YCC **46Z**, and its methyl ester **46Z-Me**.^[94] PiCC **47** binds the transition-metal ions Zn^{II}, Cd^{II}, Ni^{II}, Cu^{II}, and Pd^{II} in 1:1 complexes with high affinities and with reaction rates in the order of roughly 100 M⁻¹ s⁻¹ (Figure 28). Binding of these transition-metal ions is easily observed by a strong red-shift of the absorption bands in the visible region, for example, by $\Delta\lambda \approx 100$ nm to about $\lambda = 620$ nm for the complex **Zn-47**. Tridentate binding of the Zn^{II} ion by **47** has been deduced from NMR data in solution and a high affinity (in this case) with a linear 1:1 stoichiometry down to 1 nM solutions of Zn^{II}.^[94a] Binding at such low concentrations could be quantified by analysis of fluorescence emission. In contrast to the very weak fluorophore of **47**, the monomeric and diamagnetic complex **Zn-47** features a strong fluorescence with an emission maximum at $\lambda = 650$ nm (see Figures 27 and 28).^[94a] Coordination by such transition-metal ions restructures the *E,Z*-phyllobiladiene-*b,c* **47** to a *Z,Z*-structured and effectively tricoordinate ligand (Figure 26).^[94] In **Zn-47**, the coordinated metal ion also constrains and rigidifies the chromophore part of the ligand, thus inhibiting deactivation pathways through light-induced *E/Z* isomerization, which are presumably available to the free PiCC **47**.^[94a]

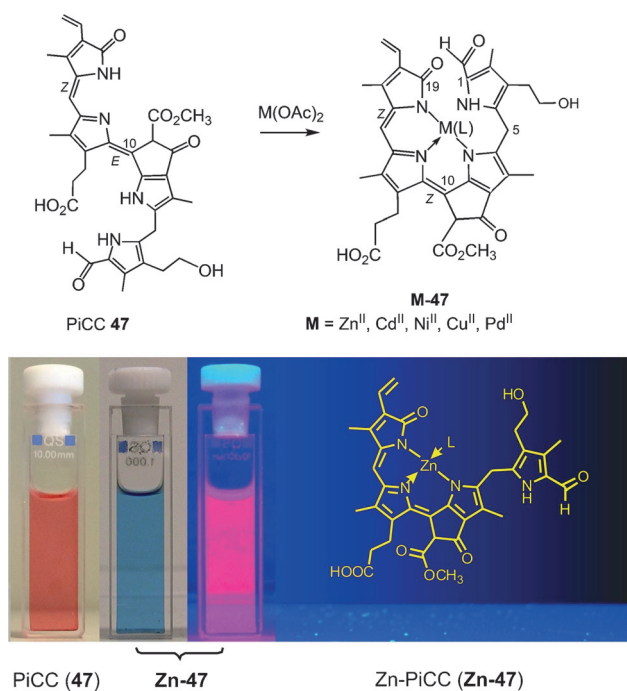


Figure 28. Complexation of transition-metal ions by PiCC **47** restructures the ligand to a Z/Z configuration and leads to blue metal complexes. **Zn-47** and **Cd-47** are complexes with closed-shell metal ions, and exhibit strong red luminescence.^[94a]

The YCC methyl ester **46Z-Me** effectively behaves as a bidentate ligand for Zn^{II} ions. ¹H NMR NOE experiments with the diamagnetic Zn complex of **46Z-Me** suggested interligand distances indicative of a 1:2 arrangement in the symmetrical complex **Zn(46Z-Me)₂** (Figure 29).^[94b,c] Similar to the situation with PiCC **47**, the binding of the closed-shell Zn^{II} ion to **46Z-Me** in DMSO solution also shifted the long-wavelength absorption maximum from $\lambda = 430$ nm to 484 nm. At the same time, the luminescence of **46Z-Me** (weak emission maximum at $\lambda = 495$ nm) was red-shifted in the complex **Zn(46Z-Me)₂**, with a maximum at $\lambda = 538$ nm, and was also intensified nearly 100-fold.^[94b] Clearly, the little-explored behavior of some of the phyllobilins, such as PiCC **47** and YCC **46Z**, in coordinating transition-metal ions indicates a considerable potential of these bilin-type ligands in binding metal ions at low concentrations and, thus, in also serving as effective indicators of the presence of metal ions.^[94a,b]

9. On the Role of Chlorophyll Breakdown in Higher Plants—Time for a New Paradigm

Having deciphered, to some extent, how Chl is degraded in some higher plants, we may now be in a better position to address the challenging question of why Chl breakdown occurs.^[9a,c] Considering the massive amounts of Chl degraded each year on Earth, the phenomenon of Chl breakdown cannot be understood as a mere visual spectacle in nature and as a priceless tourist attraction in some areas of the world.^[101]

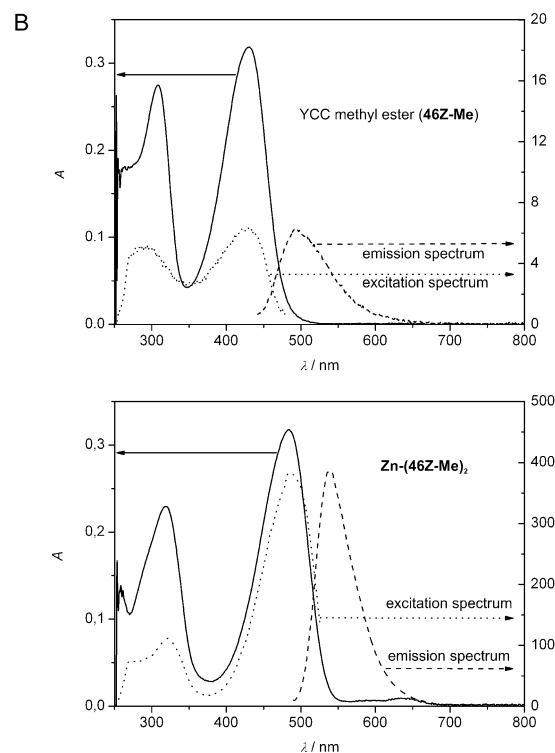
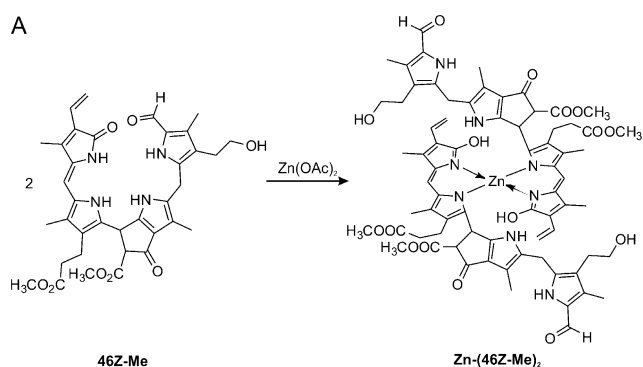


Figure 29. Binding of Zn^{II} ions to the weakly luminescent YCC methyl ester **46Z-Me** furnishes the strongly fluorescent 2:1 complex **Zn(46Z-Me)₂**.^[94b,c]

On the contrary, Chl breakdown should be considered, above all, as having beneficial consequences for the plants themselves.^[101b] Furthermore, other organisms interacting with plants may also benefit (indirectly), such as, for example, animals and humans that make use of plant-based nutrition. Therefore, and in view of the sheer amount of phyllobilins produced when Chl disappears,^[10] Chl breakdown deserves close scientific attention, not only from fundamental and applied research, but also from basic agrobiological and ecological points of view.^[9–11]

9.1. Chl Detoxification and Labilization of Proteins as Classical Roles of Chl Breakdown

In a historical interpretation, Chl breakdown was given a role in serving the direct recovery of the four nitrogen atoms of the Chl from leaves.^[2] Taking note of the now established build-up of the phyllobilins as linear tetrapyrroles, this view can, clearly, not be supported any longer.^[1a,8a,9c] However, a major direct consequence of Chl breakdown in senescent leaves is the destruction of the abundant and highly photoactive green plant pigment, thus, effectively getting rid of a cellular constituent with a strong potential as a phototoxic agent.^[9a] In addition, removal of the Chls from their proteinaceous binding partners also renders the latter more labile for proteolysis.^[102] This consequence of Chl breakdown obtained strong support from studies with “stay green” mutants (which retain their Chl), in which the relocation of proteinogenic nitrogen atom, and its recovery were found to be strongly reduced. With this knowledge, the ambivalent role of Chl breakdown in plants cannot be overestimated:^[2,5,101b] on the one hand, it eliminates the photosynthetic capacity of Chl, thus reducing a major supply line that drives metabolic activities; on the other hand, by delivering important nutrient components, such as reduced nitrogen, it contributes to enriching protein in crops and vegetables, and to the development of nutritious fruit, both of which are important from an economic point of view.^[11c,103]

9.2. On Physiological Roles of Chlorophyll Catabolites in Plants

Rather than disappearing in senescent leaves “without leaving a trace”,^[2] Chl furnishes the abundant phyllobilins. The latter, instead of being considered mere waste from Chl-detoxification,^[1a,9a] should now be given attention with respect to their possible physiological roles in plants. Strikingly, biological functions of bilin-type Chl catabolites are so far still unknown. This may, in part, be due to a lack of reliable samples of typical Chl catabolites, and to difficulties in their practical application. As a rule, phyllobilins are complex and rather unstable compounds. In this latter respect, the “persistent” *hmFCCs*^[28a] appear to represent a remarkable exception: in *hmFCCs*, the inherent tendency of FCCs to undergo isomerization to the corresponding *NCCs* is blocked (*hmFCCs* are biologically “caged” FCCs) as a consequence of a biosynthetic effort in the (banana) plant, which is seemingly useless in the absence of a further biological role.^[85]

Several phyllobilins, such as nonfluorescent type-I phyllobilins (*NCCs*), have been shown to be effective antioxidants.^[59] Likewise, *YCCs* are excellent antioxidants.^[98] Such properties of the amphiphilic phyllobilins are of considerable interest.^[59] *DNCCs*, the structurally related type-II analogues, are likely to show basically similar effects. Antioxidants are frequently abundant in plants, especially in ripe fruit,^[81a] and may be crucial for prolonging the viability of cells during senescence^[24] and ripening.^[103]

Except for the *NCCs* and *DNCCs*, most phyllobilins are classified as photoactive compounds, and may, hence, be considered relevant as cellular metabolites with the capacity

to act as light filters. Phyllochromobilins (*YCCs*, *PiCCs*, etc.) and their metal complexes could make a particularly important contribution in this respect. Thus, the colors of phyllochromobilins contribute to the pigmentation of leaves^[7] and fruit.^[51] The colors of leaves^[104] and fruit^[105] are considered to be important signals for a variety of animals. FCC fluorescence may, secondly, have a special role as optical brighteners in bananas and banana leaves^[104a,106] or act as direct fluorescence signals to animals.^[107]

FCCs are specifically efficient sensitizers of singlet oxygen ($^1\text{O}_2$): The FCC *epi-23-Me* sensitized light-induced generation of $^1\text{O}_2$ with a quantum yield of about 0.6.^[95] Clearly, the photochemical capacity of FCCs in sensitizing the formation of $^1\text{O}_2$ may play a physiological role in (senescent or ripening) plant tissue. $^1\text{O}_2$ can function in pathogen defense, as well as acting as a transiently existing signal molecule with messages for receptors in the cell nucleus.^[108] Important signals mediated by $^1\text{O}_2$ are believed to originate from chloroplasts.^[109] Photoexcited FCCs could behave as alternative production sites for $^1\text{O}_2$ in the cytosol. In light of the important roles of the transiently existing $^1\text{O}_2$ ^[110] in plants,^[108] accumulation of the persistent *hmFCCs* in ripening bananas^[28a,85] and in leaves of some other evergreens^[28b,74,76] may indicate a physiologically relevant role of FCCs as $^1\text{O}_2$ sensitizers.^[95] In line with this premise, the formation of the blue fluorescent rings around senescence-associated dark spots on the peel of ripe bananas, as a result of the local accumulation of *hmFCCs*, may have a function in detaining pathogens and in sustaining the viability of the skin tissue.^[85]

Phyllobilins have a broad capacity for acting as ligands for transition-metal complexes. The pink Chl catabolite (*PiCC*) **47** binds some transition-metal ions down to nanomolar concentrations.^[94a] Their metal-chelating ability^[94b,c] could be the basis for particular physiological roles of some phyllochromobilins in plants characterized as heavy-metal accumulators.^[111] Such plants concentrate Zn, Cd, Hg, and Ni ions in their vacuoles, where pigments, tentatively assigned as natural phyllochromobilins, were, indeed, first found.^[13c] The formation of metal complexes may, thus, be likely. Furthermore, tridentate and tripyrrolic transition-metal complexes were shown to possess druglike properties.^[112] Therefore, the capacity of *PiCCs* for binding metal ions in a tridentate fashion may be of particular relevance from plant physiological and pharmacological points of view.^[94b]

10. Summary and Outlook

In the past 25 years, research on the identity and on the chemical properties of key Chl catabolites (or phyllobilins) has provided fundamental, structure-based answers to the question of how Chl is broken down in some higher plants. Indeed, most studies have dealt with the degradation of Chl in angiosperms,^[9c] where natural Chl breakdown is inferred to follow the PaO/phyllobilin pathway. In this pathway, the monooxygenase PaO plays a key role, as it cleaves the chlorin macrocycle and generates the red, native “type-I phyllobilin”, the barely detectable *RCC*. Chl breakdown continues rapidly in the chloroplast by furnishing colorless and blue-fluorescent

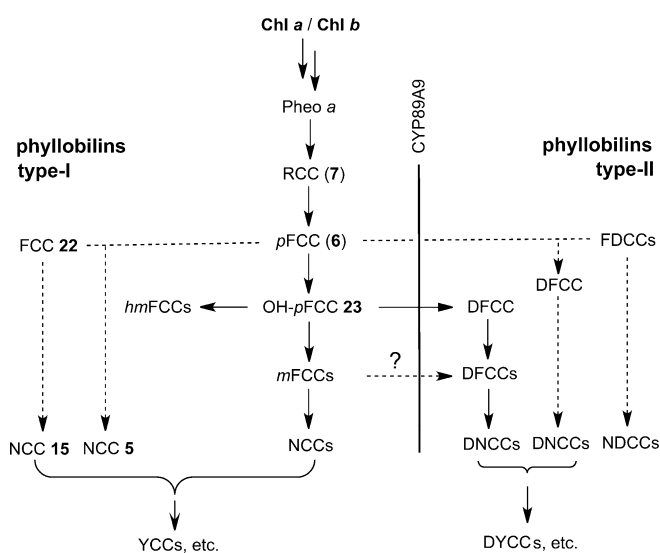


Figure 30. Abbreviated general outline of the PaO/phyllobilin pathway in some higher plants.^[10–11] Chl is broken down in a linear sequence from pheophorbide *a* (Pheo*a*) to primary FCCs (*p*FCCs). Branching out at the stage of FCCs gives several downstream lines of type-I and type-II phyllobilins. Colorless phyllobilins (NCCs and DNCCs) accumulate in senescent and ripening plant tissues. The colorless and nonfluorescent NCCs and DNCCs may be oxidized further to yellow (and then pink) phylochromobilins.

linear tetrapyrroles (FCCs). In a species-dependent way either one of the two epimeric primary FCCs (**6/epi-6**) is thereby made. At the FCC stage, the PaO/phyllobilin pathway splits into (at least) two major, and several minor downstream channels (Figure 30). This part of the catabolic pathway is mostly managed by enzymes associated with the cytosol. In some plants, one important second branch produces 1,19-dioxobilin-type (or type-II) phyllobilins by oxidative deformylation of FCCs. Chl breakdown appears to end with the transformation of fluorescent phyllobilins in the acidic vacuole into colorless, and essentially photoinactive, nonfluorescent analogues, which often accumulate in senescent leaves. However, in some plants, the typically short-lived FCCs are biosynthetically “caged” with complex ester groups and remain fluorescent as persistent hypermodified FCCs (*hm*FCCs). The accumulation of *hm*FCCs in bananas, observable by their bright blue fluorescence, is a puzzling and striking phenomenon that may be useful as a signal for fruit-eating animals.

Having learned how Chl is broken down to temporarily accumulating colorless catabolites in some higher plants, the question arises logically: What is the fate of the colorless phyllobilins? Are they broken down further in controlled metabolic processes? The recently discovered endogenous formation of phylochromobilins may play a particular role and hold a possible key to help answer this question. Current work in our laboratories is directed at finding evidence for this.

Chl breakdown has, so far, been analyzed only in a tiny fraction of the vast plant kingdom. In some investigations, naturally senescent leaves of very closely related species, such

as the deciduous apple and pear trees^[59] as well as plum and apricot trees^[68] which are all *Rosaceae*, were analyzed and showed a strongly related pattern of colorless phyllobilins. In other plants investigated, such as *A. thaliana* and related *Brassicaceae*, or in the tropical monocots *Musa acuminata* and *Spathiphyllum wallisii*, the PaO/phyllobilin pathway was discovered to produce other types of phyllobilins.

Our investigations have so far been driven by an interest in discovering the most relevant, basic types of phyllobilins in higher plants, rather than exploring the plant kingdom in a biologically systematic way. Clearly, it will be of interest to learn about Chl breakdown in (higher) plants outside the range of the angiosperms. In the specific case of the green alga *Auxenochlorella protothecoides*, the early steps of Chl breakdown are remarkably related to those of the PaO/phyllobilin pathway of higher plants.^[11a]

So far, most studies on bilin-type Chl catabolites have relied on their analysis in plant extracts. Clearly, besides such eye-opening *in vitro* studies, the observation of Chl catabolites *in vivo* may provide further insight into the effective location of processes relevant for Chl breakdown in the tissue of a leaf or a fruit. Exploratory methodological mass spectrometric^[113] and fluorescence spectroscopic studies^[85] of specific Chl catabolites have begun to pave a more systematic way to *in vivo* analyses of Chl breakdown.

In a distantly related context, exploratory studies of Chl breakdown in herbivorous protists and insects were recently reported. Thus, in the gut and digestive tract of herbivorous caterpillars, Pheo*a* was detected as the major left-over product of the ingested Chl.^[114] Furthermore, in the aquatic ecosystem, herbivorous protists were found to degrade (and detoxify) ingested Chl to a nonfluorescent cyclopheophorbide *a* enol.^[115] Clearly, the related question is no less intriguing: What happens to Chl in the metabolism of humans and higher animals?^[9d,10]

The discovery of hypermodified FCCs is particularly fascinating,^[28a] as is the broad occurrence of type-II phyllobilins as products of Chl breakdown.^[57,58] These latter 1,19-dioxobilins and the heme-derived (hemo-)bilins share substantial similarity, as they differ (mostly) only by the Chl-derived “extra” ring E of the type-II phyllobilins. Important chemical properties of the two lines of bilin-type natural products can be rather similar. Hence, phyllobilins are candidates for a variety of important biological roles, which are now an apparent domain of the (hemo-)bilins.^[116] Hence, physiological roles of phyllobilins, for example, as external signals,^[28a,117] in intra- or intercellular signaling,^[108b,118] or in plant defense, can not be discounted.^[119] In this respect, phylochromobilins may be particularly interesting experimental targets. It is truly remarkable that biological roles of the phyllobilins still wait to be discovered.

Chl breakdown is the remarkable visual sign of leaf senescence and of the ripening of some fruits. Senescence is typically associated with apoptosis, whereas ripening is not. Senescence may be caused by endogenous developmental processes^[120] or by environmental (stress) factors (such as low temperatures or the lack of light,^[121] water, or certain nutrients).^[122] A seasonal combination of several of these factors may be the underlying cause of the apparently

synchronized Chl breakdown that is observed in leaves in the fall.^[101b,123] Senescence and degreening of leaves may also be induced more locally by external factors (other than the ones listed above), such as mechanical or chemical damages, or by infections with pathogens.^[124] Plants may undergo specific responses, depending upon the means by which senescence is induced.^[125] Ripening should be seen as a basically different developmental process that is typically accompanied by Chl breakdown.^[11c] Hence, it is interesting to test the profiles of the phyllobilins formed in response to the different mechanisms that induce Chl to disappear.

Products of Chl breakdown accumulate in senescent leaves, in developing vegetables, and in ripening fruit. Their value as health-sustaining nutritional components for leaf-eating and frugivorous creatures (from insects, snails, birds, to mammals and humans), has hardly been addressed yet.^[6b,59,61,126] It is tempting, when eating apples, to consider the presence of NCCs in fruit as beneficial to our health as expressed in the old saying: “An apple a day keeps the doctor away”.^[59]

Clearly, only the tip of the iceberg of the biological phenomenon of Chl breakdown in higher plants has so far been revealed.^[6b,9c,10,11] Research on the still-elusive physiological roles of phyllobilins is mandatory, as are studies of the regulation of Chl breakdown in natural (and artificially induced) senescence and ripening, as well as investigations of the roles and interactions of Chl catabolites during the infection of plants by pathogens. The impact of the colorless phyllobilins (which are abundant in fruit and vegetables) on our health and wellbeing may be revealed by pharmacological studies. Without any doubt, the temporarily abundant remains from natural Chl breakdown leave important traces and have a fundamental impact on the biosphere of our Earth. Similar to the heme-derived bilins (the hemobilins), phyllobilins will continue to fascinate, and the “Tale of the two Bilins” may take many more years to be told.

11. Abbreviations

Chl <i>a</i>	chlorophyll <i>a</i>
Chl <i>b</i>	chlorophyll <i>b</i>
Chlide <i>a</i>	chlorophyllide <i>a</i>
DCC	dioxobilin-type Chl catabolite
DFCC	dioxobilin-type FCC
DNCC	dioxobilin-type NCC
DYCC	dioxobilin-type YCC
FCC	type-I fluorescent Chl catabolite
FDCC	fluorescent DCC
NCC	type-I nonfluorescent Chl catabolite
NDCC	nonfluorescent DCC
Pheina	pheophytin <i>a</i>
Pheoa	pheophorbide <i>a</i>
PiCC	type-I pink Chl catabolite
RCC	red Chl catabolite
YCC	type-I yellow Chl catabolite

Acknowledgements

I would like to thank Thomas Müller and my co-workers in Innsbruck (Chengjie Li, Matthias Roiser, Mathias Scherl, Gerhard Scherzer, Iris Süssenbacher, and Clemens Vergeiner) as well as their previous colleagues, for their excellent research contributions to the present topic. I am also grateful to Thomas and Clemens for the graphics contribution, and to Stefan Hörtensteiner and Michael Oberhuber and their groups (at the University of Zürich and at the Versuchszentrum Laimburg, Italy, respectively) for very fruitful collaborations. Our work has been supported by the Austrian Science Fund (FWF project Nos. P 19596, L-472, and I-563) and by the Interreg IV Italy-Austria program (ERDF; project “Biophytiro”, ID Nr. 5345).

How to cite: *Angew. Chem. Int. Ed.* **2016**, *55*, 4882–4907
Angew. Chem. **2016**, *128*, 4964–4990

- [1] a) B. Kräutler, P. Matile, *Acc. Chem. Res.* **1999**, *32*, 35–43; b) A. Morel in *Chlorophylls and Bacteriochlorophylls. Biochemistry Biophysics, Functions and Applications* (Eds.: B. Grimm, R. Porra, W. Rüdiger, H. Scheer), *Adv. Photosynth. Res.*, Vol. 25, Springer, Dordrecht, **2006**, S. 521–534.
- [2] G. A. F. Hendry, J. D. Houghton, S. B. Brown, *New Phytol.* **1987**, *107*, 255–302.
- [3] H. Falk, *Chemistry of Linear Oligopyrroles and Bile Pigments*, Springer, Wien, **1989**.
- [4] a) S. B. Brown, K. M. Smith, G. M. F. Bisset, R. F. Troxler, *J. Biol. Chem.* **1980**, *255*, 8063–8068; b) S. B. Brown, J. D. Houghton, G. A. F. Hendry in *Chlorophylls* (Ed.: H. Scheer), CRC, Boca Raton, USA, **1991**, pp. 465–489.
- [5] P. Matile, *Chimia* **1987**, *41*, 376–381.
- [6] a) B. Kräutler, *Photochem. Photobiol. Sci.* **2008**, *7*, 1114–1120; b) S. Moser, T. Müller, M. Oberhuber, B. Kräutler, *Eur. J. Org. Chem.* **2009**, 21–31.
- [7] S. Moser, M. Ulrich, T. Müller, B. Kräutler, *Photochem. Photobiol. Sci.* **2008**, *7*, 1577–1581.
- [8] a) B. Kräutler, B. Jaun, K. Bortlik, M. Schellenberg, P. Matile, *Angew. Chem. Int. Ed. Engl.* **1991**, *30*, 1315–1318; *Angew. Chem.* **1991**, *103*, 1354–1357; b) B. Kräutler, B. Jaun, W. Amrein, K. Bortlik, M. Schellenberg, P. Matile, *Plant Physiol. Biochem.* **1992**, *30*, 333–346.
- [9] a) P. Matile, S. Hörtensteiner, H. Thomas, B. Kräutler, *Plant Physiol.* **1996**, *112*, 1403–1409; b) B. Kräutler, S. Hörtensteiner in *Chlorophylls and Bacteriochlorophylls. Biochemistry Biophysics, Functions and Applications* (Eds.: B. Grimm, R. Porra, W. Rüdiger, H. Scheer), *Adv. Photosynth. Res.*, Vol. 25, Springer, Dordrecht, **2006**, S. 237–260; c) S. Hörtensteiner, B. Kräutler, *Biochim. Biophys. Acta Bioenergetics* **2011**, *1807*, 977–988; d) B. Kräutler, S. Hörtensteiner in *Handbook of Porphyrin Science*, Vol. 28 (Eds.: G. C. Ferreira, K. M. Kadish, K. M. Smith, R. Guilard), World Scientific Publishing, Singapore, **2013**, pp. 117–185.
- [10] B. Kräutler, *Chem. Soc. Rev.* **2014**, *43*, 6227–6238.
- [11] a) S. Hörtensteiner, *Plant Mol. Biol.* **2013**, *82*, 505–517; b) R. Tanaka, A. Tanaka, *Biochim. Biophys. Acta Bioenergetics* **2011**, *1807*, 968–976; c) C. S. Barry, *Plant Sci.* **2009**, *176*, 325–333.
- [12] a) H. Nakamura, B. Musicki, Y. Kishi, O. Shimomura, *J. Am. Chem. Soc.* **1988**, *110*, 2683–2685; b) H. Nakamura, Y. Kishi, O. Shimomura, D. Morse, J. W. Hastings, *J. Am. Chem. Soc.* **1989**, *111*, 7607–7611.
- [13] a) P. Matile, S. Ginsburg, M. Schellenberg, H. Thomas, *J. Plant Physiol.* **1987**, *129*, 219–228; b) H. Thomas, K. Bortlik, D. Rentsch, M. Schellenberg, P. Matile, *New Phytol.* **1989**, *111*, 3–

- 8; c) P. Matile, S. Ginsburg, M. Schellenberg, H. Thomas, *Proc. Natl. Acad. Sci. USA* **1988**, *85*, 9529–9532.
- [14] K. Bortlik, C. Peisker, P. Matile, *J. Plant Physiol.* **1990**, *136*, 161–165.
- [15] C. Peisker, H. Thomas, F. Keller, P. Matile, *J. Plant Physiol.* **1990**, *136*, 544–549.
- [16] a) H. M. Schiebel, H. R. Schulten, *Mass Spectrom. Rev.* **1986**, *5*, 249–311; b) T. Matsuo, R. M. Caprioli, M. L. Gross, Y. Seyama, *Biological Mass Spectrometry Present and Future*, Wiley, New York, **1994**; c) T. Müller, S. Vergeiner, B. Kräutler, *Int. J. Mass Spectrom.* **2014**, *365–366*, 48–55.
- [17] a) R. R. Ernst, G. Bodenhausen, A. Wokaun, *Principles of Nuclear Magnetic Resonance in One & Two Dimensions*, Clarendon Press, Oxford, **1987**; b) H. Kessler, M. Gehrke, C. Griesinger, *Angew. Chem. Int. Ed. Engl.* **1988**, *27*, 490–536; *Angew. Chem.* **1988**, *100*, 507–554.
- [18] a) W. Mühlecker, B. Kräutler, S. Ginsburg, P. Matile, *Helv. Chim. Acta* **1993**, *76*, 2976–2980; b) NCCs (and other Chl catabolites) were typically given convenient provisional names, first, with reference to the plant of their origin, e.g. as Hv-NCC, when from barley (*Hordeum vulgare*), or as Bn-NCC, when from oilseed rape (*Brassica napus*).^[19,22] NCCs were indexed according to their relative polarity (as Bn-NCC-1, Bn-NCC-2, etc.), as determined by reversed-phase HPLC. This naming was frequently found inadequate, and retention times (min) observed under the conditions of a standard HPLC protocol were later introduced as an index, e.g. Sw-NCC-58 for an NCC with a standard retention time of 58 min from *Sp. wallisii*.^[10,74]
- [19] See, Section 1.2. for the now recommended semisystematic nomenclature of linear tetrapyrrolic Chl catabolites based on the structure of phytylbilanes (**1**).^[10]
- [20] a) M. Oberhuber, J. Berghold, K. Breuker, S. Hörtensteiner, B. Kräutler, *Proc. Natl. Acad. Sci. USA* **2003**, *100*, 6910–6915; b) M. Oberhuber, J. Berghold, B. Kräutler, *Angew. Chem. Int. Ed.* **2008**, *47*, 3057–3061; *Angew. Chem.* **2008**, *120*, 3100–3104; c) previously, NCCs and other ring-opened Chl catabolites were named in another semisystematic, structure-based way as derivatives of phytylporphyrin.^[21] Thus, **1** was named a 3¹,3²,8²-trihydroxy-1,4,5,10,15,20-(22*H*,24*H*)-octahydro-13²-[methoxycarbonyl]-4,5-dioxo-4,5-secophytoporphyrate.^[8a]
- [21] a) P. R. Ortiz de Montellano, K. Auclair in *The Porphyrin Handbook*, Vol. 12 (Eds.: K. M. Kadish, K. M. Smith, R. Guilard), Academic Press, Amsterdam, **2003**, pp. 183–210; b) A. Wilks in *Tetrapyrroles: Birth, Life and Death* (Eds.: M. J. Warren, A. G. Smith), Landes Bioscience, Austin, Texas, **2008**, pp. 101–115.
- [22] H. Scheer in *Chlorophylls and Bacteriochlorophylls. Biochemistry Biophysics, Functions and Applications* (Eds.: B. Grimm, R. Porra, W. Rüdiger, H. Scheer), *Adv. Photosynth. Res.*, Vol. 25, Springer, Dordrecht, **2006**, S. 1–26.
- [23] W. Mühlecker, B. Kräutler, *Plant Physiol. Biochem.* **1996**, *34*, 61–75.
- [24] P. Matile in *Advances in Botanical Research*, Vol. 25 (Ed.: J. A. Callow), Academic Press, New York, **1997**, pp. 87–112.
- [25] W. Mühlecker, K. H. Ongania, B. Kräutler, P. Matile, S. Hörtensteiner, *Angew. Chem. Int. Ed. Engl.* **1997**, *36*, 401–404; *Angew. Chem.* **1997**, *109*, 401–404.
- [26] a) I. Süssenbacher, B. Christ, S. Hörtensteiner, B. Kräutler, *Chem. Eur. J.* **2014**, *20*, 87–92; b) I. Süssenbacher, C. Kreutz, B. Christ, S. Hörtensteiner, B. Kräutler, *Chem. Eur. J.* **2015**, *21*, 11664–11670; c) I. Süssenbacher, S. Hörtensteiner, B. Kräutler, *Angew. Chem. Int. Ed.* **2015**, *54*, 13777–13781; *Angew. Chem.* **2015**, *127*, 13981–13985.
- [27] B. Christ, I. Süssenbacher, S. Moser, N. Bichsel, A. Egert, T. Müller, B. Kräutler, S. Hörtensteiner, *Plant Cell* **2013**, *25*, 1868–1880.
- [28] a) S. Moser, T. Müller, M.-O. Ebert, S. Jockusch, N. J. Turro, B. Kräutler, *Angew. Chem. Int. Ed.* **2008**, *47*, 8954–8957; *Angew. Chem.* **2008**, *120*, 9087–9091; b) S. Banala, S. Moser, T. Müller, C. Kreutz, A. Holzinger, C. Lütz, B. Kräutler, *Angew. Chem. Int. Ed.* **2010**, *49*, 5174–5177; *Angew. Chem.* **2010**, *122*, 5300–5304.
- [29] S. Hörtensteiner, F. Vicentini, P. Matile, *New Phytol.* **1995**, *129*, 237–246.
- [30] P. Folly, N. Engel, *J. Biol. Chem.* **1999**, *274*, 21811–21816.
- [31] A. Tanaka, R. Tanaka, *Curr. Opin. Plant Biol.* **2006**, *9*, 248–255.
- [32] a) V. Scheumann, S. Schoch, W. Rüdiger, *Planta* **1999**, *209*, 364–370; b) H. Ito, T. Ohtsuka, A. Tanaka, *J. Biol. Chem.* **1996**, *271*, 1475–1479.
- [33] W. Rüdiger, B. Grimm in *Chlorophylls and Bacteriochlorophylls. Biochemistry Biophysics, Functions and Applications* (Eds.: B. Grimm, R. Porra, W. Rüdiger, H. Scheer), *Adv. Photosynth. Res.*, Vol. 25, Springer, Dordrecht, **2006**, S. 133–146.
- [34] T. Azoulay Shemer, S. Harpaz-Saad, E. Belausov, N. Lovat, O. Krokhin, V. Spicer, K. G. Standing, E. E. Goldschmidt, Y. Eyal, *Plant Physiol.* **2008**, *148*, 108–118.
- [35] Y. Shioi, N. Tomita, T. Tsuchiya, K. Takamiya, *Plant Physiol. Biochem.* **1996**, *34*, 41–47.
- [36] a) D. Amir-Shapira, E. E. Goldschmidt, A. Altman, *Proc. Natl. Acad. Sci. USA* **1987**, *84*, 1901–1905; b) L. Guyer, S. S. Hofstetter, B. Christ, B. S. Lira, M. Rossi, S. Hörtensteiner, *Plant Physiol.* **2014**, *166*, 44–56.
- [37] S. Schelbert, S. Aubry, B. Burla, B. Agne, F. Kessler, K. Krupinska, S. Hörtensteiner, *Plant Cell* **2009**, *21*, 767–785.
- [38] P. Matile, B. Kräutler, *Chem. Unserer Zeit* **1995**, *29*, 298–306.
- [39] a) T. Düggelein, K. Bortlik, H. Gut, P. Matile, H. Thomas, *Physiol. Plant.* **1988**, *74*, 131–136; b) T. Düggelein, M. Schellenberg, K. Bortlik, P. Matile, *J. Plant Physiol.* **1988**, *133*, 492–497.
- [40] M. Barber, R. S. Bordoli, G. J. Elliott, R. D. Sedgwick, A. N. Tyler, *Anal. Chem.* **1982**, *54*, A645–A650.
- [41] A. Gossauer, N. Engel, *J. Photochem. Photobiol. B* **1996**, *32*, 141–151.
- [42] B. Kräutler, W. Mühlecker, M. Anderl, B. Gerlach, *Helv. Chim. Acta* **1997**, *80*, 1355–1362.
- [43] a) J. Iturraspe, A. Gossauer, *Tetrahedron* **1992**, *48*, 6807–6812; b) K. M. Smith, in *Chlorophylls* (Ed.: H. Scheer), CRC, Boca Raton, FL, **1991**, pp. 115–144.
- [44] S. Rodoni, W. Mühlecker, M. Anderl, B. Kräutler, D. Moser, H. Thomas, P. Matile, S. Hörtensteiner, *Plant Physiol.* **1997**, *115*, 669–676.
- [45] A. Pružinska, G. Tanner, I. Anders, M. Roca, S. Hörtensteiner, *Proc. Natl. Acad. Sci. USA* **2003**, *100*, 15259–15264.
- [46] S. Hörtensteiner, K. L. Wüthrich, P. Matile, K. H. Ongania, B. Kräutler, *J. Biol. Chem.* **1998**, *273*, 15335–15339.
- [47] W. Mühlecker, B. Kräutler, D. Moser, P. Matile, S. Hörtensteiner, *Helv. Chim. Acta* **2000**, *83*, 278–286.
- [48] S. Rodoni, F. Vicentini, M. Schellenberg, P. Matile, S. Hörtensteiner, *Plant Physiol.* **1997**, *115*, 677–682.
- [49] a) S. Hörtensteiner, S. Rodoni, M. Schellenberg, F. Vicentini, O. I. Nandi, Y. L. Qui, P. Matile, *Plant Biol.* **2000**, *2*, 63–67; b) K. L. Wüthrich, L. Bovet, P. E. Hunziker, I. S. Donnison, S. Hörtensteiner, *Plant J.* **2000**, *21*, 189–198.
- [50] J. Berghold, K. Breuker, M. Oberhuber, S. Hörtensteiner, B. Kräutler, *Photosynth. Res.* **2002**, *74*, 109–119.
- [51] S. Moser, T. Müller, A. Holzinger, C. Lütz, B. Kräutler, *Chem. Eur. J.* **2012**, *18*, 10873–10885.
- [52] N. Frankenberg, K. Mukougawa, T. Kohchi, J. C. Lagarias, *Plant Cell Physiol.* **2001**, *13*, 965–978.
- [53] M. Sugishima, Y. Kitamori, M. Noguchi, T. Kohchi, K. Fukuyama, *J. Mol. Biol.* **2009**, *389*, 376–387.
- [54] M. Sugishima, Y. Okamoto, M. Noguchi, T. Kohchi, H. Tamiaki, K. Fukuyama, *J. Mol. Biol.* **2010**, *402*, 879–891.

- [55] M. Oberhuber, B. Kräutler, *ChemBioChem* **2002**, *3*, 104–107.
- [56] T. Dammeyer, N. Frankenberger-Dinkel, *Photochem. Photobiol. Sci.* **2008**, *7*, 1121–1130.
- [57] F. G. Losey, N. Engel, *J. Biol. Chem.* **2001**, *276*, 8643–8647.
- [58] T. Müller, M. Rafelsberger, C. Vergeiner, B. Kräutler, *Angew. Chem. Int. Ed.* **2011**, *50*, 10724–10727; *Angew. Chem.* **2011**, *123*, 10912–10916.
- [59] T. Müller, M. Ulrich, K.-H. Ongania, B. Kräutler, *Angew. Chem. Int. Ed.* **2007**, *46*, 8699–8702; *Angew. Chem.* **2007**, *119*, 8854–8857.
- [60] A. Pruzinska, G. Tanner, S. Aubry, I. Anders, S. Moser, T. Müller, K.-H. Ongania, B. Kräutler, J.-Y. Youn, S. J. Liljegen, S. Hörtensteiner, *Plant Physiol.* **2005**, *139*, 52–63.
- [61] M. Roiser, T. Müller, B. Kräutler, *J. Agric. Food Chem.* **2015**, *63*, 1385–1392.
- [62] J. Berghold, C. Eichmüller, S. Hörtensteiner, B. Kräutler, *Chem. Biodiversity* **2004**, *1*, 657–668.
- [63] C. Curty, N. Engel, *Phytochemistry* **1996**, *42*, 1531–1536.
- [64] M. Oberhuber, J. Berghold, W. Mühlecker, S. Hörtensteiner, B. Kräutler, *Helv. Chim. Acta* **2001**, *84*, 2615–2627.
- [65] J. Berghold, T. Müller, M. Ulrich, S. Hörtensteiner, B. Kräutler, *Monatsh. Chem.* **2006**, *137*, 751–763.
- [66] T. Müller, S. Moser, K. H. Ongania, A. Pruzinska, S. Hörtensteiner, B. Kräutler, *ChemBioChem* **2006**, *7*, 40–42.
- [67] B. Christ, S. Schelbert, S. Aubry, I. Süßenbacher, T. Müller, B. Kräutler, S. Hörtensteiner, *Plant Physiol.* **2012**, *158*, 628–641.
- [68] T. Erhart, C. Vergeiner, G. Scherzer, C. Mittelberger, P. Robatscher, M. Oberhuber, B. Kräutler, Unpublished Results.
- [69] M. Scherl, T. Müller, R. G. Huber, C. Kreutz, E. Zass, K. R. Liedl, B. Kräutler, Unpublished Results.
- [70] S. Hörtensteiner, *Phytochemistry* **1998**, *49*, 953–956.
- [71] A. Eschenmoser, *Angew. Chem. Int. Ed. Engl.* **1988**, *27*, 5–39; *Angew. Chem.* **1988**, *100*, 5–40.
- [72] C. Li, K. Wurst, B. Kräutler, Unpublished Results.
- [73] T. Müller, R. Treichel, B. Kräutler, Unpublished Results.
- [74] B. Kräutler, S. Banala, S. Moser, C. Vergeiner, T. Müller, C. Lütz, A. Holzinger, *FEBS Lett.* **2010**, *584*, 4215–4221.
- [75] D. Lafont, F. Carriere, F. Ferrato, P. Boullanger, *Carbohydr. Res.* **2006**, *341*, 695–704.
- [76] C. Vergeiner, S. Banala, B. Kräutler, *Chem. Eur. J.* **2013**, *19*, 12294–12305.
- [77] C. Vergeiner, B. Kräutler, Unpublished Results.
- [78] a) N. Djapic, A. Djuric, A. Pavlovic, *Res. J. Agr. Sci.* **2009**, *41*, 256–260; b) G. Scherzer, B. Kräutler, Unpublished Results.
- [79] a) P. R. Ortiz de Montellano, *Cytochrome P450—Structure, Mechanisms, and Biochemistry*, 3rd ed., Kluwer Academic, New York, **2004**, p. 689; b) I. G. Denisov, T. M. Makris, S. G. Sligar, I. Schlichting, *Chem. Rev.* **2005**, *105*, 2253–2277.
- [80] M. Gregory, P. J. Mak, S. G. Sligar, J. R. Kincaid, *Angew. Chem. Int. Ed.* **2013**, *52*, 5342–5345; *Angew. Chem.* **2013**, *125*, 5450–5453.
- [81] a) G. B. Seymour, M. Poole, J. J. Giovannoni, G. A. Tucker, *The Molecular Biology and Biochemistry of Fruit Ripening*, Wiley-Blackwell, Malaysia, **2013**; b) B. W. Shirley, *Trends Plant Sci.* **1996**, *1*, 377–382.
- [82] J. J. Ríos, A. Pérez-Gálvez, M. Roca, *Food Res. Int.* **2014**, *65*, 255–262.
- [83] J. J. Ríos, M. Roca, A. Pérez-Gálvez, *J. Agric. Food Chem.* **2014**, *62*, 10576–10584.
- [84] A. J. Keys, C. L. Leaver, D. H. R. Barton, B. D. Brown, D. A. Widdowson, *Nature* **1971**, *232*, 423–424.
- [85] S. Moser, T. Müller, A. Holzinger, C. Lütz, S. Jockusch, N. J. Turro, B. Kräutler, *Proc. Natl. Acad. Sci. USA* **2009**, *106*, 15538–15542.
- [86] We became interested in knowing what different test persons remember from their direct visual impression of freshly ripe bananas illuminated with 360 nm UV light in a dark room. A test with over 40 different test persons of various age groups was carried out at the University of Innsbruck. While a blue color was observed by all of them, as recorded by the test persons immediately after leaving the dark room, there is a significant spread from person to person of the actual intensity as well as of the hue of the blue color. Blue fluorescent rings around senescence-associated dark spots on the peel of overripe bananas can be observed (even more) easily in darkened rooms.
- [87] F. Mendoza, J. M. Aguilera, *J. Food Sci.* **2004**, *69*, E471–E477.
- [88] R. Choehom, S. Ketsa, W. G. van Doorn, *Postharvest Biol. Technol.* **2004**, *31*, 167–175.
- [89] M. Ulrich, S. Moser, T. Müller, B. Kräutler, *Chem. Eur. J.* **2011**, *17*, 2330–2334.
- [90] D. A. Lightner, *Bilirubin: Jekyll and Hyde Pigment of Life*, Springer, Wien, **2013**.
- [91] C. Vergeiner, M. Ulrich, C. Li, X. Liu, T. Müller, B. Kräutler, *Chem. Eur. J.* **2015**, *21*, 136–149.
- [92] M. Scherl, T. Müller, B. Kräutler, *Chem. Biodiversity* **2012**, *9*, 2605–2617.
- [93] D. Wakana, H. Kato, T. Momose, N. Sasaki, Y. Ozeki, Y. Goda, *Tetrahedron Lett.* **2014**, *55*, 2982–2985.
- [94] a) C. Li, M. Ulrich, X. Liu, K. Wurst, T. Müller, B. Kräutler, *Chem. Sci.* **2014**, *5*, 3388–3395; b) C. Li, B. Kräutler, *Dalton Trans.* **2015**, *44*, 10116–10127; c) C. Li, K. Wurst, B. Kräutler, *J. Porph. Phthal.* **2016**, in press.
- [95] S. Jockusch, N. J. Turro, S. Banala, B. Kräutler, *Photochem. Photobiol. Sci.* **2014**, *13*, 407–411.
- [96] A. Eschenmoser, *Chem. Soc. Rev.* **1976**, *5*, 377–410.
- [97] R. Stocker, Y. Yamamoto, A. F. McDonagh, A. N. Glazer, B. N. Ames, *Science* **1987**, *235*, 1043–1046.
- [98] M. Ulrich, B. Kräutler, Unpublished Results, see M. Ulrich, PhD thesis, University of Innsbruck **2011**.
- [99] a) A. R. Battersby, *Nat. Prod. Rep.* **2000**, *17*, 507–526; b) B. Kräutler, *Chimia* **1987**, *41*, 277–292; c) B. Kräutler, B. Jaun in *Concepts and Models in Bioinorganic Chemistry* (Eds.: H.-B. Kraatz, N. Metzler-Nolte), Wiley-VCH, Weinheim, **2006**, S. 177–212; d) *Handbook of Porphyrin Science, Vol. 1–30* (Eds.: K. M. Kadish, K. M. Smith, R. Guilard), World Scientific Publication, Singapore, **2010**; e) K. M. Smith, *Porphyrins and Metalloporphyrins*, Elsevier Science, Amsterdam, **1975**.
- [100] a) A. L. Balch, F. L. Bowles in *Handbook of Porphyrin Science, Vol. 8* (Eds.: K. M. Kadish, K. M. Smith, R. Guilard), World Scientific Publishing, Singapore, **2010**, pp. 293–342; b) M. Bröring in *Handbook of Porphyrin Science, Vol. 8* (Eds.: K. M. Kadish, K. M. Smith, R. Guilard), World Scientific Publishing, USA, **2010**, pp. 343–501.
- [101] a) C. R. Bell, A. H. Lindsey, *Fall Colors and Woodland Harvests*, Laurel Hill Press, Chapel Hill, USA, **1990**; b) P. Matile, *Exp. Gerontol.* **2000**, *35*, 145–158; c) P. O. Lim, H. J. Kim, H. G. Nam, *Annu. Rev. Plant Biol.* **2007**, *58*, 115–136.
- [102] a) P. Matile, S. Hörtensteiner, H. Thomas, *Annu. Rev. Plant Physiol. Plant Mol. Biol.* **1999**, *50*, 67–95; b) B. Hauck, A. P. Gay, J. Macduff, C. M. Griffiths, H. Thomas, *Plant Cell Environ.* **1997**, *20*, 1007–1018.
- [103] J. Giovannoni, *Annu. Rev. Plant Physiol. Plant Mol. Biol.* **2001**, *52*, 725–749.
- [104] a) E. W. Stiles, *Am. Nat.* **1982**, *120*, 500–509; b) M. Archetti, S. P. Brown, *Proc. R. Soc. London Ser. B* **2004**, *271*, 1219–1223.
- [105] a) M. Archetti, *Proc. R. Soc. London Ser. B* **2009**, *276*, 2575–2580; b) E. Cazetta, H. M. Schaefer, M. Galetti, *Evol. Ecol.* **2009**, *23*, 233–244; c) D. Osorio, A. C. Smith, M. Vorobyev, H. M. Buchanan-Smith, *Am. Nat.* **2004**, *164*, 696–708.
- [106] H. Zollinger, *Color Chemistry*, 3rd ed., Wiley-VCH, Zürich & Weinheim, **2003**.
- [107] a) K. E. Arnold, I. P. F. Owens, N. J. Marshall, *Science* **2002**, *295*, 92–92; b) C. H. Mazel, T. W. Cronin, R. L. Caldwell, N. J.

- Marshall, *Science* **2004**, *303*, 51–51; c) M. L. M. Lim, M. F. Land, D. Li, *Science* **2007**, *315*, 481–481; d) F. Hausmann, K. E. Arnold, N. J. Marshall, I. P. F. Owens, *Proc. R. Soc. London Ser. B* **2003**, *270*, 61–67.
- [108] a) D. Wagner, D. Przybyla, R. O. D. Camp, C. Kim, F. Landgraf, K. P. Lee, M. Wursch, C. Laloi, M. Nater, E. Hideg, K. Apel, *Science* **2004**, *306*, 1183–1185; b) C. Triantaphylidès, M. Havaux, *Trends Plant Sci.* **2009**, *14*, 219–228; c) J. P. Knox, A. D. Dodge, *Phytochemistry* **1985**, *24*, 889–896.
- [109] M. J. Terry, A. G. Smith, *Front. Plant Sci.* **2013**, *4*, 1–14.
- [110] P. R. Ogilby, *Chem. Soc. Rev.* **2010**, *39*, 3181–3209.
- [111] U. Krämer, *Annu. Rev. Plant Biol.* **2010**, *61*, 517–534.
- [112] A. Fürstner, *Angew. Chem. Int. Ed.* **2003**, *42*, 3582–3603; *Angew. Chem.* **2003**, *115*, 3706–3728.
- [113] T. Müller, S. Oradu, D. R. Ifa, R. G. Cooks, B. Kräutler, *Anal. Chem.* **2011**, *83*, 5754–5761.
- [114] A. Badgaa, J. Aiqun, R. Büchler, K. Ploss, W. Boland, *J. Chem. Ecol.* **2014**, *40*, 1232–1240.
- [115] a) Y. Kashiyama, A. Yokoyama, Y. Kinoshita, S. Shoji, H. Miyashiya, T. Shiratori, H. Suga, K. Ishikawa, A. Ishikawa, I. Inouye, K.-i. Ishida, D. Fujinuma, K. Aoki, M. Kobayashi, S. Nomoto, T. Mizoguchi, H. Tamiaki, *Proc. Natl. Acad. Sci. USA* **2012**, *109*, 17328–17335; b) H. Falk, G. Hoornaert, H. P. Isenring, A. Eschenmoser, *Helv. Chim. Acta* **1975**, *58*, 2347–2357.
- [116] N. Frankenberg, J. C. Lagarias in *The Porphyrin Handbook*, Vol. 13 (Eds.: K. M. Kadish, K. M. Smith, R. Guilard), Elsevier Science Oxford, UK, **2003**, pp. 211–235.
- [117] P. Sumner, J. D. Mollon, *J. Exp. Biol.* **2000**, *203*, 1987–2000.
- [118] a) J. Chory, *Plant J.* **2010**, *61*, 982–991; b) M. Heil, J. Ton, *Trends Plant Sci.* **2008**, *13*, 264–272.
- [119] a) N. Eckardt, *Plant Cell* **2008**, *20*, 241–243; b) H. H. Felle, A. Herrmann, P. Schäfer, R. Hüchelhoven, K.-H. Kogel, *J. Plant Physiol.* **2008**, *165*, 52–59.
- [120] a) S. Balazadeh, S. Parlitz, B. Mueller-Roeber, R. C. Meyer, *Plant Biol.* **2008**, *10*, 136–147; b) A. M. Price, D. F. A. Orellana, F. M. Salleh, R. Stevens, R. Acock, V. Buchanan-Wollaston, A. D. Stead, H. J. Rogers, *Plant Physiol.* **2008**, *147*, 1898–1912; c) H. Zhang, C. Zhou, *Plant Mol. Biol.* **2012**, *82*, 539–545.
- [121] L. M. Weaver, R. M. Amasino, *Plant Physiol.* **2001**, *127*, 876–886.
- [122] B. B. Buchanan, W. Gruissem, R. L. Jones, *Biochemistry & Molecular Biology of Plants*, American Society of Plant Physiologists, Rockville, USA, **2001**.
- [123] J. Keskitalo, G. Bergquist, P. Gardestrom, S. Jansson, *Plant Physiol.* **2005**, *139*, 1635–1648.
- [124] a) J. T. Greenberg, A. Guo, D. F. Klessig, F. M. Ausubel, *Cell* **1994**, *77*, 551–563; b) J. T. Greenberg, N. Yao, *Cell Microbiol.* **2004**, *6*, 201–211.
- [125] a) V. Buchanan-Wollaston, *J. Exp. Bot.* **1997**, *48*, 181–199; b) J. L. Dangl, R. A. Dietrich, H. Thomas in *Biochemistry & Molecular Biology of Plants* (Eds.: B. B. Buchanan, W. Gruissem, R. L. Jones), American Society of Plant Physiologists, Rockville, MD, USA, **2001**, pp. 1044–1100.
- [126] M. Roca, *Food Chem.* **2012**, *130*, 134–138.

Received: September 23, 2015

Published online: February 26, 2016